more than 70 bp, fragments with a *Bam*HI digestion site were determined as target candidates, since the fragments amplified by SMART RACE-PCR included *Bam*HI recognition site at the 5′ end of exon 12 of the *RET* gene. All fragments in Figure 1A–D that could be recognized as a band were confirmed to be digested with *Bam*HI. As shown in lanes 2–4 of Figure 1A and C, PCR products looked like smears without clear and intense bands when adaptor concentration was high (2–10 μM). PCR products with 0.2–1 μM of SMART adaptor revealed an obvious and intense band of more than 70 bp compared with the bands at other higher concentrations (lanes 5–7, Fig. 1A and C, indicated by asterisks), though the sizes of these target candidate fragments differed somewhat among various concentrations of SMART adaptor. Treatment with 0.1 μM of SMART adaptor showed that amplified bands of more than 70 bp in length were observed only infrequently (lane 8, Fig. 1A, C).

Addition timing of SMART adaptor

When cDNA was synthesized in the presence of SMART adaptor (2–10 μM), electrophoretic images of PCR products were similar to those in the case of addition of adaptor after completion of the cDNA synthesis (compare lanes 2–4 in Fig. 1B and D with lanes 2–4 in Fig. 1A and C). When cDNA was prepared in the presence of a lower concentration (0.2–1 μM) of SMART adaptor, the electrophoretic patterns differed from those where adaptor was added after completion of cDNA synthesis (compare lanes 5–7 in Fig. 1B and D with lanes 5–7 in Fig. 1A and C, respectively). Namely, weak bands of more than 70 bp were observed (lanes 5–7, Fig. 1B, D). Although treatment with 0.1 μM of SMART adaptor occasionally produced clear and intense bands (lane 8, Fig. 1B, indicated by an arrow), amplified bands of more than 70 bp in length were rarely observed (lane 8, Fig. 1D).

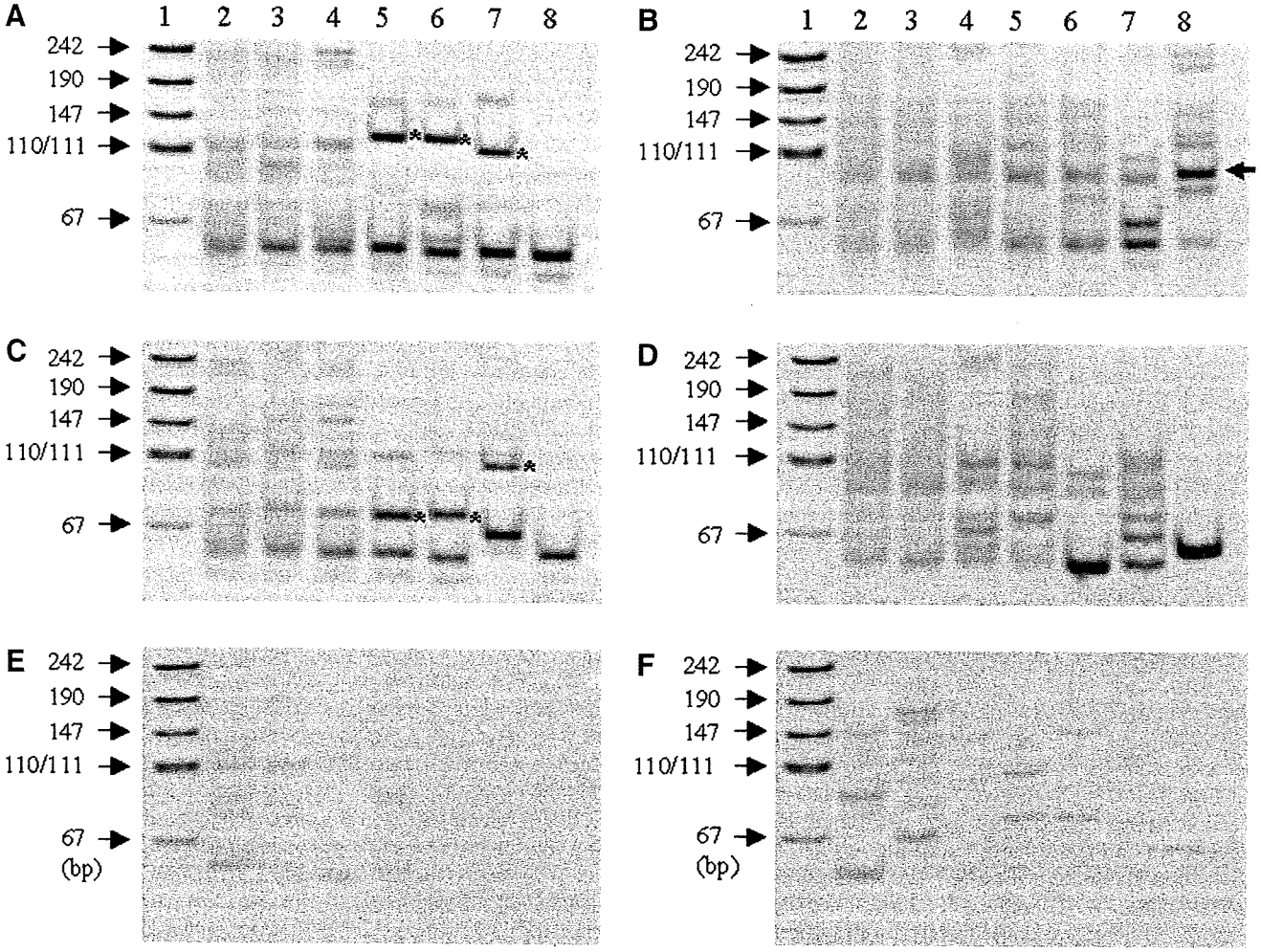

FIG. 1. Effects of concentration and addition timing of SMART adaptor on improved SMART RACE-PCR amplification. (**A, B**) SMART RACE-PCR products with total RNA from specimen with *RET/PTC1*. (**C, D**) SMART RACE-PCR products with total RNA from specimen with *RET/PTC3*. (**E, F**) SMART RACE-PCR products with total RNA that revealed no detectable expression of the *RET* gene tyrosine kinase domain. (**A, C, E**) reveal RACE-PCR products when various concentrations of SMART adaptor were added after completion of cDNA synthesis (lane 2, 10 μM; lane 3, 5 μM; lane 4, 2 μM; lane 5, 1 μM; lane 6, 0.4 μM; lane 7, 0.2 μM; lane 8, 0. 1 μM). Lane 1 indicates pUC19-*Msp*I digest for DNA size marker. (**B, D, F**) indicate RACE-PCR products when cDNA was synthesized in the presence of SMART adaptor. The asterisks and arrow indicate clear and intense candidate fragments measuring more than 70 bp. PCR, polymerase chain reaction; RACE, 5′ rapid amplification of cDNA ends; SMART, switching mechanism at 5′ end of RNA transcript.

When RNA extracted from archival samples with no detectable expression of *RET* gene TK domain was used, several weak bands were observed regardless of the addition timing of SMART adaptor. However, few bands (more than 70 bp) were found in the cases of 0.1, 0.2, or 0.4 μM of SMART adaptor (lanes 6–8, Fig. 1E, F). Not all weak bands in Figure 1E and F could be digested with *Bam*HI. No bands were observed when H_2O was used as template for RACE-PCR. In addition, SMART RACE-PCR without reverse transcription produced no amplified bands whatsoever.

Incubation time

We examined the effects of incubation time after addition of adaptor on amplification by SMART RACE-PCR using RNA from specimens with *RET/PTC1*. After SMART adaptor was added to cDNA solution to give a final concentration of 0.2 μM, the reaction was incubated for various durations at 42°C. Among target candidate bands of about 90 bp (lanes 2–6, Fig. 2, indicated by asterisks) found in SMART RACE-PCR products until 45 minutes of incubation time, a case treated for 45 minutes revealed the most intense band (lane 6, Fig. 2). Incubation for 60 minutes resulted in a larger intense target candidate band (lane 7, Fig. 2) than did other incubation times. In the case of 90-minute incubation (lane 8, Fig. 2), the larger candidate band disappeared and a weak 90 bp candidate band reappeared (indicated by an asterisk).

We next examined how efficiently cDNA fragments of the target gene can be isolated by this improved SMART RACE method. Target candidate bands of about 100 bp (lane 7, Fig. 1A) and 90 bp (lane 7, Fig. 1C) in the second PCR products were eluted from 8% acrylamide gel and cloned onto a pUC118 plasmid vector. Plasmid DNA with a longer insert than 70 bp was sequenced. As shown in Table 2, all 36 screened colonies proved to be plasmid DNA harboring *RET/PTC1* fragments of 97 bp in length. *RET/PTC3* fragments with a length of 89 bp were also detected in 35 out of 36 colonies, as shown in Table 2. This suggests that almost all candidate fragments amplified by the improved SMART RACE method are actually target cDNA fragments.

RET/PTC8 *in thyroid cancer tissue from A-bomb survivors*

RNA was extracted from unbuffered formalin-fixed, paraffin-embedded papillary thyroid cancer tissue specimens from 64 subjects exposed to A-bomb radiation, and *BCR* gene expression was detected in 52 of the 64 cases. Among these 52 cases, 11 showed expression of *RET* gene TK domain, of which 9 cases had *RET/PTC1* or *RET/PTC3*, as shown in Table 3. Two papillary thyroid cancer cases showing no

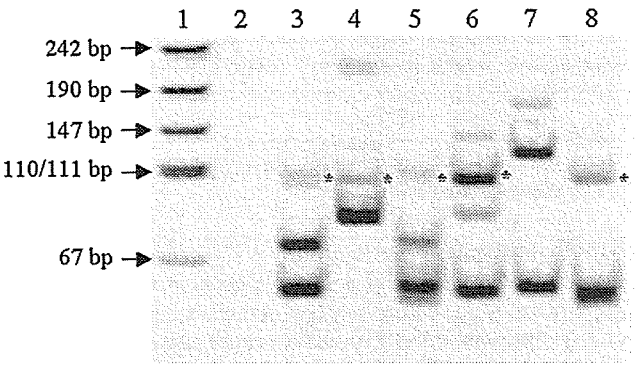

FIG. 2. Effect of incubation time on improved SMART RACE-PCR amplification. The reaction was incubated for various times at 37°C after SMART adaptor was added to cDNA solution to give a final concentration of 0.05 μM (lane 2, 0 minute; lane 3, 10 minutes; lane 4, 20 minutes; lane 5, 30 minutes; lane 6, 45 minutes; lane 7, 60 minutes; lane 8, 90 minutes). Lane 1 indicates pUC19-*Msp*I digest for DNA size marker. The asterisks indicate fragments of about 90 bp with *Bam*HI recognition site.

RET/PTC1 or *RET/PTC3* rearrangement were examined for type of rearrangement using this improved SMART RACE method. The target band in the second PCR products (Fig. 3A, indicated by an arrow) was eluted and cloned into a cloning vector. Since 23 out of 24 white colonies contained plasmid DNA with *Bam*HI site and a longer insert than about 70 bp, plasmid DNA in the 23 colonies was sequenced. The sequencing of the portion upstream of *RET* exon 12 found in all clones was identical to the 5′ part of the kinectin 1 gene, whose insert length was 93 bp (Fig. 3B). As shown in Figure 3C, the band corresponding to *RET/PTC8* was also detected in the papillary thyroid cancer specimen from the same A-bomb survivor by RT-PCR. Further, the improved SMART RACE method enabled us to identify a novel rearrangement of the *RET* gene in papillary thyroid cancer of another A-bomb survivor. This new type of *RET/PTC*, whose partner gene is acyl coenzyme A binding domain 5 (*ACBD5*) located on chromosome 10p, is now being analyzed for its tumorigenicity. Expression of the *ACBD5-RET* fusion gene was confirmed in RNA from the cancer specimens by RT-PCR (Fig. 3C).

Discussion

RACE reaction with RNA extracted from fresh tissues or cells can be easily and successfully performed using the SMART RACE kit (Clontech). On the other hand, as far as we know, there are thus far no reports on RACE with RNA extracted from archival unbuffered formalin-fixed,

TABLE 2. ACCURACY OF TARGET cDNA FRAGMENT AMPLIFIED BY IMPROVED SWITCHING MECHANISM AT 5′ END OF RNA TRANSCRIPT 5′ RAPID AMPLIFICATION OF cDNA ENDS METHOD

	No. of screened white color colonies	*No. of* Bam*HI-positive colonies*	*No. of confirmation by sequencing*	*Efficiency (%)*
No 1[a]	36	36	36	100
No 2[b]	36	36	35[c]	97

[a]Thyroid cancer with *RET/PTC1*.
[b]Thyroid cancer with *RET/PTC3*.
[c]One clone failed to perform sequencing.

TABLE 3. NUMBER OF CASES EXPOSED TO ATOMIC BOMB RADIATION IN THIS STUDY

Total tested	BCR *positive*	RET-TK *positive*	RET/PTC1 *positive*	RET/PTC8 *positive*	ACBD5-RET *positive*
64	52	11	9[a]	1	1

[a]One case carried both *RET/PTC1* and *RET/PTC3*.
TK, tyrosine kinase.

paraffin-embedded tissue samples. We succeeded in identification and isolation of a partner gene of rearranged *RET* using RNA extracted from archival unbuffered formalin-fixed and paraffin-embedded thyroid cancer tissue specimens by improved SMART RACE method. A series of experiments from cDNA synthesis to PCR was conducted at least three times. Similar electrophoresis patterns could be reproduced, though the sizes of the target bands differed somewhat. Size differences of amplified fragments between experiments may largely have been due to degradation of RNA extracted from archival samples, since such a phenomenon was not observed when cDNA was prepared with the random primer (9 mer) using intact RNA from fresh samples (data not shown).

We found that the SMART RACE method enabled isolation of 5′ upstream fragments in target cDNA with RNA extracted from archival formalin-fixed, paraffin-embedded tissue specimens by adjusting the concentration and the timing of the addition of SMART adaptor. The optimal concentration of SMART adaptor (ultimately around 0.2 μM) was lower than that in conventional SMART RACE with oligo (dT) using intact RNA (9). This finding was contrary to our expectation that a higher concentration of adaptor would be required because of degradation of the RNA extracted from archival formalin-fixed and paraffin-embedded tissue. Since a large amount of SMART adaptor brought in by cDNA used as a PCR template has a GGG sequence at the 3′ end, this adaptor

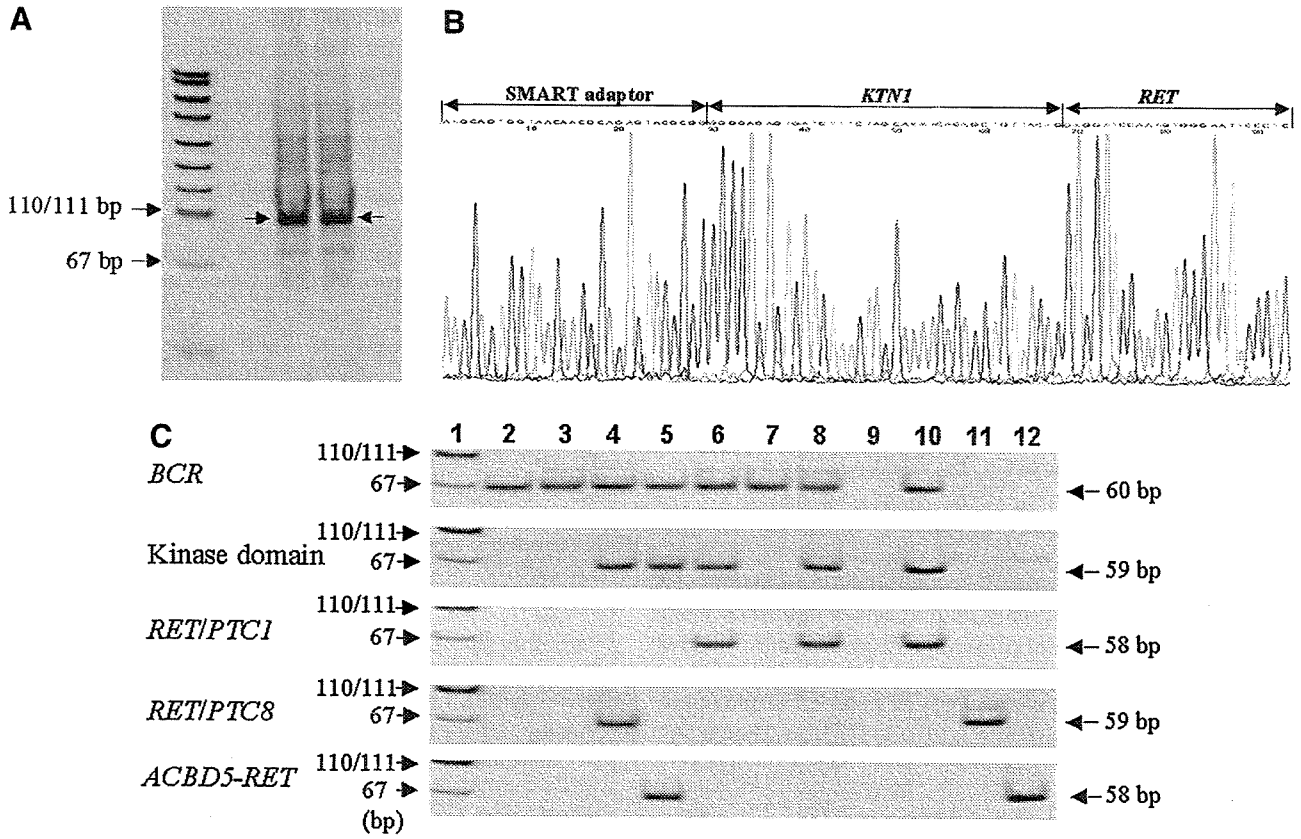

FIG. 3. Identification of *RET/PTC8* in papillary thyroid cancer from one A-bomb survivor. (**A**) Second PCR products of RNA extracted from an archival formalin-fixed, paraffin-embedded papillary thyroid cancer specimen from an A-bomb survivor (arrows indicate the target band in the second PCR products). (**B**) Sequence of *RET/PTC8* isolated by this improved SMART RACE method. (**C**) Expression of *RET/PTC8* (RT-PCR product) in papillary thyroid cancer in the A-bomb survivor. Lanes 2–8 indicate RT-PCR products from RNA in papillary thyroid cancer specimens of A-bomb survivors. Lanes 2, 3, and 7 show no detectable expression of *RET* tyrosine kinase domain; lane 4, *RET/PTC8*; lane 5, *ACBD5-RET*; lanes 6 and 8, *RET/PTC1*; lane 9, H_2O for negative control; lane 10, cell line TPC1 harboring *RET/PTC1*; lane 11, genomic DNA plus 77 base-synthesized nucleotides (PTC8-oligo77) for positive control of *RET/PTC8*; lane 12, genomic DNA plus 77 base-synthesized nucleotides (ACBD-RET-oligo77) for positive control of *ACBD5-RET*. Lane 1 indicates pUC19-*Msp*I digest for DNA size marker. A-bomb, atomic bomb; RT, reverse transcription.

may cause nonspecific amplification by the first PCR. As a result, specific and efficient RT-PCR may be hindered. Further, when cDNA in the presence of SMART adaptor was prepared with random primers (9 mer) using RNA extracted from archival tissue specimens, we could not obtain the clear and intense target candidate bands observed in the case of addition of adaptor after completion of cDNA synthesis (Fig. 1A and C vs. 1B and D). However, when cDNA was prepared with random primers using intact total RNA, target candidate bands could be detected regardless of the timing of adding SMART adaptor (data not shown). This suggests that when degraded RNA was used, a larger amount of short cDNA primed with SMART adaptor may be produced, possibly interfering with specific PCR amplification.

In addition to the concentration and the timing of the addition of SMART adaptor, length of incubation time was also an important factor for efficient amplification by our SMART RACE-PCR: optimal incubation time was relatively long (45–60 minutes) despite addition of adaptor after cDNA synthesis completion. Thus, although amplification efficiency by SMART RACE-PCR largely depended on concentration of SMART adaptor, timing of adaptor addition, and incubation time when cDNA was prepared with random primer using RNA extracted from archival formalin-fixed and paraffin-embedded tissue specimens, unlike SMART RACE with intact RNA, we found that the improved SMART RACE method achieved successful isolation of 5′ upstream fragments in target cDNA with RNA extracted from archival unbuffered formalin-fixed, paraffin-embedded tissue specimens.

A rare rearrangement of the *RET* gene, *RET/PTC8*, previously identified in papillary thyroid cancers in children from areas contaminated by the Chernobyl accident (12), was detected in papillary thyroid cancer of one A-bomb survivor exposed to more than 2 Gy of radiation. Further, a novel rearrangement of the *RET* gene (*ACBD5-RET* fusion gene) was identified in papillary thyroid cancer of another A-bomb survivor exposed to more than 1.5 Gy. It is interesting to note that a rare *RET/PTC8* rearrangement and a novel *ACBD5-RET* fusion gene were identified in papillary thyroid cancers in A-bomb survivors exposed to a relatively high radiation dose.

Since this improved SMART RACE method achieves effective amplification of the unknown 5′ upstream region of certain genes with even 10 ng of total RNA extracted from archival formalin-fixed and paraffin-embedded tissue specimens, the method is expected to prove useful in molecular analyses using archival tissue samples of limited quantity.

Acknowledgments

The RERF, Hiroshima and Nagasaki, Japan, is a private, nonprofit foundation funded by Japan's Ministry of Health, Labour, and Welfare and the U.S. Department of Energy, the latter in part through the National Academy of Sciences. This publication was supported by RERF Research Protocols RP 5–02 and B31-03, and in part by a Grant-in-Aid for Science Research from the Ministry of Education, Culture, Sports, Science, and Technology, and a Grant-in-Aid for Cancer Research from Japan's Ministry of Health, Labour, and Welfare.

Disclosure Statement

The authors declare that they have no commercial associations that might create a conflict of interest in connection with this article.

References

1. Mies C 1994 Molecular biological analysis of paraffin-embedded tissues. Hum Pathol **25**:550–560.
2. Suárez HG 1998 Genetic alterations in human epithelial thyroid tumors. Clin Endocrinol **48**:531–546.
3. Tallini G, Asa SL 2001 RET oncogene activation in papillary thyroid carcinoma. Adv Anat Pathol **8**:345–354.
4. Ciampi R, Nikiforov YE 2007 RET/PTC rearrangements and BRAF mutations in thyroid tumorigenesis. Endocrinology **148**:936–941.
5. Saenko V, Rogounovitch T, Shimizu-Yoshida Y, Abrosimov A, Lushnikov E, Roumiantsev P, Matsumoto N, Nakashima M, Meirmanov S, Ohtsuru A, Namba H, Tsyb A, Yamashita S 2003 Novel tumorigenic rearrangement, *Δrfp/ret*, in a papillary thyroid carcinoma from externally irradiated patient. Mutat Res **527**:81–90.
6. Arighi E, Borrello MG, Sariola H 2005 RET tyrosine kinase signaling in development and cancer. Cytokine Growth Factor Rev **16**:441–467.
7. Ciampi R, Giordano TJ, Wikenheiser-Brokamp K, Koenig RJ, Nikiforov YE 2007 *HOOK3-RET*: a novel type of *RET/PTC* rearrangement in papillary thyroid carcinoma. Endocr-Relat Cancer **14**:445–452.
8. Chenchik A, Zhu YY, Diatchenko L, Li R, Hill J, Siebert PD 1998 Generation and use of high quality cDNA from small amounts of total RNA by SMART PCR. In: Siebert PD, Larrick JW (eds) RT-PCR Methods for Gene Cloning and Analysis. Eaton Publishing, Natick, MA, pp 305–319.
9. Zhu YY, Machleder EM, Chenchik A, Li R, Siebert PM 2001 Reverse transcriptase template switching: a SMART™ approach for full-length cDNA library construction. BioTechniques **30**:892–897.
10. Frohman MA, Dush MK, Martin GR 1988 Rapid production of full-length cDNAs from rare transcripts: amplification using a single gene-specific oligonucleotide primer. Proc Natl Acad Sci USA **85**:8998–9002.
11. Hamatani K, Eguchi H, Takahashi K, Koyama K, Mukai M, Ito R, Taga M, Yasui W, Nakachi K 2006 Improved RT-PCR amplification for molecular analyses with long-term preserved formalin-fixed, paraffin-embedded tissue specimens. J Histochem Cytochem **54**:773–780.
12. Salassidis K, Bruch J, Zitzelsberger H, Lengfelder E, Kellerer AM, Bauchinger M 2000 Translocation t(10;14)(q11.2;q22.1) fusing the kinectin to the *RET* gene creates a novel rearranged form (PTC8) of the *RET* proto-oncogene in radiation-induced childhood papillary thyroid carcinoma. Cancer Res **60**:2786–2789.

Address correspondence to:
Kiyohiro Hamatani, Ph.D.
Department of Radiobiology/Molecular Epidemiology
Radiation Effects Research Foundation
5-2 Hijiyama Park, Minami-ku
Hiroshima-shi
Hiroshima 732-0815
Japan

E-mail: hamatani@rerf.or.jp

Carcinogenesis vol.30 no.12 pp.2037–2041, 2009
doi:10.1093/carcin/bgp247
Advance Access publication October 20, 2009

Lung cancer susceptibility among atomic bomb survivors in relation to CA repeat number polymorphism of *epidermal growth factor receptor* gene and radiation dose

Kengo Yoshida*, Kei Nakachi, Kazue Imai, John B.Cologne[1], Yasuharu Niwa, Yoichiro Kusunoki and Tomonori Hayashi

Department of Radiobiology/Molecular Epidemiology and [1]Department of Statistics, Radiation Effects Research Foundation, 5-2 Hijiyama Park, Minami Ward, Hiroshima City 732-0815, Japan

*To whom correspondence should be addressed. Tel: +81 82 261 3131; Fax: +81 82 261 3170; Email: kyoshi@rerf.or.jp

Lung cancer is a leading cause of cancer death worldwide. Prevention could be improved by identifying susceptible individuals as well as improving understanding of interactions between genes and etiological environmental agents, including radiation exposure. The epidermal growth factor receptor (EGFR)-signaling pathway, regulating cellular radiation sensitivity, is an oncogenic cascade involved in lung cancer, especially adenocarcinoma. The cytosine adenine (CA) repeat number polymorphism in the first intron of *EGFR* has been shown to be inversely correlated with EGFR production. It is hypothesized that CA repeat number may modulate individual susceptibility to lung cancer. Thus, we carried out a case–cohort study within the Japanese atomic bomb (A-bomb) survivor cohort to evaluate a possible association of CA repeat polymorphism with lung cancer risk in radiation-exposed or negligibly exposed (<5 mGy) A-bomb survivors. First, by dividing study subjects into *Short* and *Long* genotypes, defined as the summed CA repeat number of two alleles ≤37 and ≥38, respectively, we found that the *Short* genotype was significantly associated with an increased risk of lung cancer, specifically adenocarcinoma, among negligibly exposed subjects. Next, we found that prior radiation exposure significantly enhanced lung cancer risk of survivors with the *Long* genotype, whereas the risk for the *Short* genotype did not show any significant increase with radiation dose, resulting in indistinguishable risks between these genotypes at a high radiation dose. Our findings imply that the EGFR pathway plays a crucial role in assessing individual susceptibility to lung adenocarcinoma in relation to radiation exposure.

Introduction

Despite focused research over decades, lung cancer remains a leading cause of cancer deaths worldwide as well as in Japan (1). Effective prevention of lung cancer could be improved by identifying susceptible individuals as well as seeking a comprehensive understanding of lung carcinogenesis and potentially causal environmental agents. It is conceivable that lung cancer risk is influenced by low-penetrance genetic variation, which may contribute to gene–environment interactions (2,3). Causal environmental factors include cigarette smoking and other factors, including exposure to ionizing radiation (4–6). Epidemiological studies on atomic bomb (A-bomb) survivors conducted by the Radiation Effects Research Foundation (RERF) have revealed a radiation dose-dependent increase in incidence of certain cancers, especially lung cancer (7).

Few molecular epidemiology studies have assessed interindividual variation in radiation sensitivity in relation to lung cancer development among A-bomb survivors. Our previous study showed that large interindividual variation in somatic mutability in response to prior A-bomb irradiation was associated with subsequent development of all cancers combined, in terms of erythrocyte *glycophorin A*-mutant frequency, which suggests the existence of genetic factors involved in radiation sensitivity and cancer susceptibility (8). Considering the implications of those results, we began searching for gene polymorphisms that might be responsible for individual susceptibility to radiation-associated lung cancer.

The initial event in the development of lung adenocarcinoma is thought to be alteration of the epidermal growth factor receptor (*EGFR*) gene (9). Mutations in *EGFR* are frequently observed in patients with lung adenocarcinoma (10,11). Gene amplification of *EGFR* is also frequently observed in patients with adenocarcinoma as well as squamous cell carcinoma of the lung, resulting in enhanced EGFR levels that lead to poor clinical prognosis and a chemo/radioresistant phenotype (9,12,13). Therefore, the altered EGFR-signaling pathway, which turns on downstream pathways such as Ras-Raf-Mek and PI3K-Akt, is thought to contribute to the development of non-small-cell lung cancer in general through enhanced cell proliferation, inhibition of apoptosis, invasion and metastasis (4,9).

It is noteworthy that EGFR signaling facilitates cellular resistance to radiation exposure and that EGFR and its signaling cascade are induced by radiation exposure even in the absence of ligand binding (12,14,15). EGFR is thought to be a key molecule in the development of lung cancer in the general population as well as that of radiation-associated lung cancer found in A-bomb survivors. We therefore conducted a case–cohort study within a cohort of A-bomb survivors to assess the relationship between a functional polymorphism of *EGFR* and radiation-associated lung cancer.

The 5′-regulatory sequence of *EGFR* contains two functional gene polymorphisms that are markedly associated with the transcriptional activity of this gene: −216G/T and a highly polymorphic microsatellite sequence consisting of cytosine adenine (CA)-dinucleotide repeats (16,17). In this study, we focused on the CA repeat polymorphism in the first intron of *EGFR* because −216G/T variant alleles are infrequent in Asian populations (16,18). The number of CA repeats also shows substantial variation by ethnicity; larger numbers are found in East Asians than in persons of European descent or African-Americans (18–20). As demonstrated by *in vitro* and *in vivo* studies, CA repeat number is inversely correlated with messenger RNA or protein expression (21–23). Consequently, the association between CA repeat number and risk of various cancers has been examined by several groups, although the results on lung cancer have been inconsistent (24,25). This study aims to address: (i) whether *EGFR* CA repeat number is associated with risk of lung cancer development in the Japanese population who had not been exposed to A-bomb irradiation and (ii) how prior exposure to A-bomb irradiation influences the risk of radiation-associated lung cancer among A-bomb survivors in conjunction with the CA repeat polymorphism.

Subjects and methods

Study subjects

RERF's predecessor research organization, the Atomic Bomb Casualty Commission, established two major cohort studies to assess the health effects of A-bomb radiation exposure (26): the Life Span Study started in 1950 with ~120 000 members in Hiroshima and Nagasaki, including 93 000 A-bomb survivors and the Adult Health Study (AHS) including ~23 000 members who were selected from the Life Span Study and received biennial medical examinations beginning in 1958. The Immunology Study began in the AHS cohort in December 1981 with the aim of investigating radiation effects on the immune systems of A-bomb survivors; blood samples to examine immune-related biomarkers were collected from 9385 AHS participants who visited RERF for medical examinations and who donated blood samples for this study in 1981–2006. Additionally, 7131 persons among the 9385 AHS participants

Abbreviations: A-bomb, atomic bomb; AHS, Adult Health Study; CA, cytosine adenine; EGFR, epidermal growth factor receptor; Gy, Gray; PCR, polymerase chain reaction; RERF, Radiation Effects Research Foundation; RR, relative risk.

donated blood samples (peripheral lymphocytes and/or blood absorbed on paper disks) from which DNA could be extracted.

A total of 4764 participants were selected for the Immunogenome cohort study to assess relationships between cancer development and gene polymorphisms among A-bomb survivors, focusing on immune-related genes. The inclusion criteria were as follows: age <80 years at the time of blood collection; radiation dose information available; no prior cancer diagnosis at the time of blood collection and informed consent given for extracting and using DNA for research purposes (living members) or approval of the RERF Ethics Committee for Genome Research (deceased members who died prior to giving informed consent). Among the 4764 cohort members, 1061 incident cancers were identified from the Hiroshima and Nagasaki Tumor Registries, diagnosed between 1981 and 2001. Those included cancers of the stomach (n = 227), colon (n = 165), rectum (n = 53), liver (n = 115), lung (n = 124), breast (n = 90) and thyroid (n = 47).

Within the cohort, we defined a sub-cohort for this case–cohort study consisting of 2160 members who were randomly selected, a sampling rate of 0.45. A total of 486 incident cancers, including 62 lung cancer cases, were included in this sub-cohort. Cases were all 124 members who were diagnosed with lung cancer between 1981 and 2001. Their time of entry into the cohort was the year when the blood donation for the Immunology Study was first made. By histological type of lung cancer, the cases consisted of 66 (52.4%) adenocarcinomas, 21 (16.7%) squamous cell carcinomas, 10 (7.9%) small cell carcinomas and 29 (23.0%) other types including large cell carcinomas. In addition, two multiple cancer cases were included; those histological types were counted individually. This study was approved by the RERF Ethics Committee for Genome Research.

Determination of CA repeat number

The number of polymorphic CA repeats in the first intron of *EGFR* was determined by polymerase chain reaction (PCR)-based fragment length analysis using fluorescent primers along with DNA direct sequencing (18,24). First, genomic DNA was extracted from peripheral blood cells with proteinase K digestion and a QIAamp DNA Mini Kit (QIAGEN, Hilden, Germany) and subjected to whole genome amplification (GenomiPhi DNA Amplification Kit, GE Healthcare, Little Chalfont, Buckinghamshire, UK). Then, 50–200 ng of the amplified DNA was used for PCR with both carboxyfluorescein fluorochrome-labeled and unlabeled forward primers (5′-GGGCTCACAGCAAACTTCTC-3′) and unlabeled reverse primers (5′-AAGCCAGACTCGCTCATGTT-3′). The 10 μl PCR reaction mixture contained 10× PCR buffer (Sigma–Aldrich, St Louis, MO), 0.5 U Taq DNA polymerase (Sigma–Aldrich), 0.2 mM each of deoxynucleoside triphosphate, 2 mM $MgCl_2$, 200 nM each unlabeled primer and 20 nM labeled primer. PCR cycle conditions consisted of an initial denaturation step at 94°C for 5 min followed by 40 cycles of 30 s at 94°C, 30 s at 65°C and 60 s at 72°C, with a final elongation step at 72°C for 5 min. After 1 μl of PCR product and 0.5 μl Genescan 500 ROX molecular weight standard (Applied Biosystems, Foster City, CA) were denatured in 10 μl deionized formamide, the number of CA repeats was determined using an ABI 3100 genetic analyzer (Applied Biosystems) and GeneMapper software (version 3.0, Applied Biosystems). The exact number of CA repeats was verified by DNA direct sequencing with 16 and 18 repeat homozygote samples.

Statistical analysis

The data were sampled according to the case–cohort design, which does not require a rare disease assumption (27). The unweighted case–cohort approach was used for analysis (28). Relative risks for cancer incidence were estimated using the Cox proportional hazard model in terms of either follow-up time (years) or age as the underlying time axis. Analyses were performed with SPSS (version 14.0, SPSS, Chicago, IL).

All models included adjustment for age at the time of blood collection, gender, city (Hiroshima versus Nagasaki), smoking status (number of cigarettes per day) and radiation dose. Information on smoking was collected at the time of blood collection. A-bomb radiation dose in Gray (Gy) was estimated using the DS02 dosimetry system (29), based on weighted skin dose computed as the gamma dose plus 10 times the neutron dose. A radiation dose <0.005 Gy was called non-exposed when performing analyses based on dose group.

Results

Table I shows characteristics of cases and sub-cohort members. Cases evidenced higher proportions of males, smokers and persons with the highest radiation doses compared with sub-cohort members.

PCR-based identification of CA repeat number revealed a frequency distribution ranging between 9 and 24, with a bimodal pattern having peaks at 16 (16.6%) and 20 (61.9%) among non-exposed members in the sub-cohort (Figure 1A). The allele distribution showed close agreement with those from Asian populations as previously reported (19,24). The allele distributions of lung cancer cases and sub-cohort members were compared for the radiation non-exposed population (Figure 1A) or radiation exposed population (Figure 1B). In the non-exposed population, a relative frequency of 16 CA repeats or 20 CA repeats in cases was higher or lower, respectively, than that in sub-cohort members (Figure 1A). On the other hand, there was no substantial difference in relative frequency of 16 CA repeats or 20 CA repeats between exposed cases and exposed sub-cohort members (Figure 1B). In contrast to the differences in cases by radiation exposure status, no distinguishable difference was found between the non-exposed and exposed sub-cohort members.

Table I. Characteristics of the study population within the RERF AHS cohort

	Cases	Sub-cohort
Total[a]	124 (100)	2160 (100)
Age at entry[b]	59 (48–74)	56 (41–75)
Gender[a]		
Men	68 (54.8)	779 (36.1)
Women	56 (45.2)	1381 (63.9)
City[a]		
Hiroshima	84 (67.7)	1432 (66.3)
Nagasaki	40 (32.3)	728 (33.7)
Smoking status[a]		
Non-smoker	49 (39.5)	1571 (72.7)
Smoker	64 (51.6)	511 (23.6)
Unknown	11 (8.9)	78 (3.6)
Radiation dose[a]		
<5 mGy	41 (33.1)	906 (41.9)
5–712[c]	37 (29.8)	627 (29.0)
≥712	46 (37.1)	627 (29.0)
Histological type[d]		
Adenocarcinoma	66 (52.4)	
Squamous cell carcinoma	21 (16.7)	
Small cell carcinoma	10 (7.9)	
Other types	29 (23.0)	

[a]Number (%).
[b]Median (5–95% percentiles).
[c]712 mGy: median dose in exposed sub-cohort members.
[d]Two multiple primary cancer cases are included (one is adenocarcinoma and adenosquamous carcinoma, the other is adenocarcinoma and small cell carcinoma). Those histological types are counted individually.

In the analysis to calculate lung cancer risk, we used two methods to genotype the CA repeat polymorphism according to previous studies (25,30): method 1 sums repeat numbers of two alleles in each individual and defines his or her genotype as *Long* (sum ≥38) or *Short* (sum ≤37) (Figure 2); method 2 defines the two alleles separately as *long* (allele repeat number ≥18) or *short* (repeat number ≤17) and combines them for each individual as *long/long*, *long/short* or *short/short*. We report the results from method 1 genotyping in the text (for results from method 2 genotyping, refer supplementary Tables SI–SIII, available at *Carcinogenesis* Online).

As a preliminary to risk estimation, we confirmed that age, gender, city, smoking status and radiation dose did not influence the distribution of the CA repeat number in the sub-cohort population (data not shown). First, overall relative risk (RR) of lung cancer for the *Short* genotype in all subjects was evaluated by Cox regression analysis with adjustment for age, gender, city, smoking and radiation dose, taking the *Long* genotype as a reference: a significant increase in risk was found for the *Short* genotype (RR: 1.79, 95% CI: 1.14–2.82, Table II).

Next, we stratified the subjects by radiation dose (<5, 5–712 and ≥712 mGy) and evaluated the relative risks for the genotypes using two models: risk ratios for the genotypes within the same dose group (without considering radiation effects on risk) and relative risks for

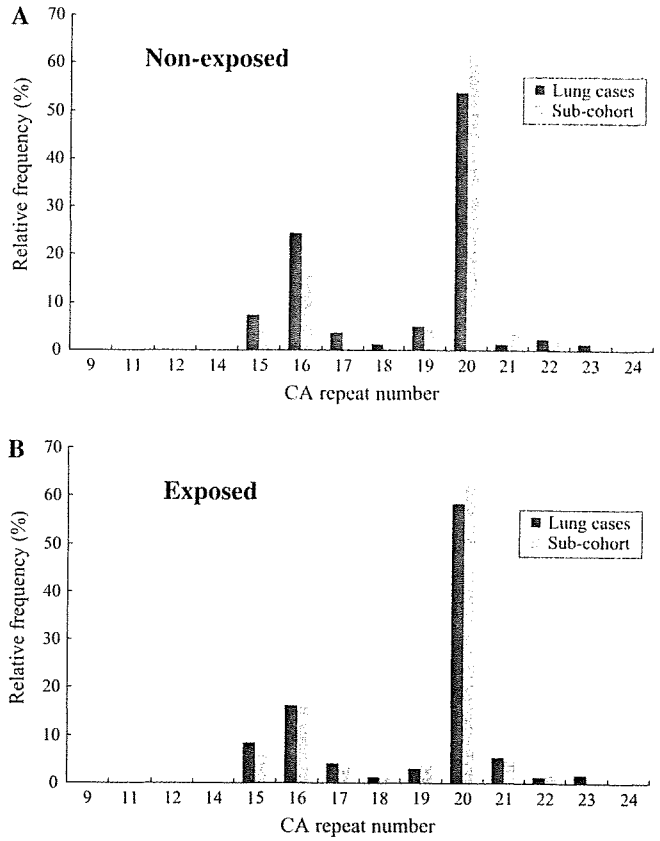

Fig. 1. Relative allele frequencies of the *EGFR* CA repeat polymorphism. (**A**) Radiation non-exposed (<5 mGy) lung cancer cases (N = 82 chromosomes) and sub-cohort members (N = 1812). (**B**) Radiation-exposed (≥5 mGy) lung cancer cases (N = 166) and sub-cohort members (N = 2 508).

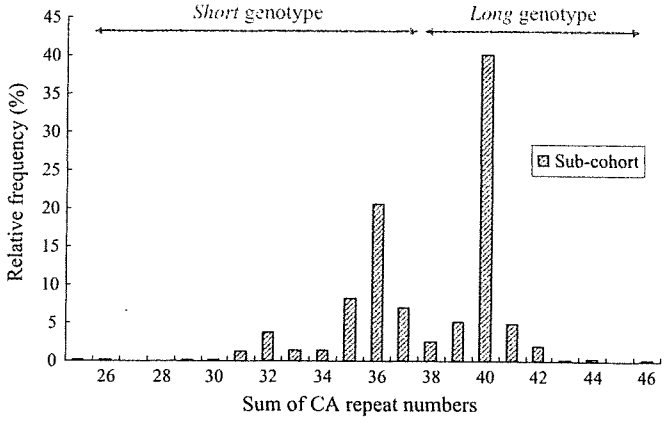

Fig. 2. Relative frequencies of summed CA repeat numbers in each individual in radiation non-exposed (<5m Gy) sub-cohort members; N = 906 (individuals). Genotype definition in the genotyping method 1 is indicated at the top of the graph.

the genotypes as functions of radiation dose (*Long* genotype in the non-exposed population used as a reference). When looking at risk ratios (RR1 in Table III), the *Short* genotype revealed a significantly increased risk of lung cancer in the non-exposed population (RR: 2.43, 95% CI: 1.23–4.79), but this genetic effect on risk disappeared in the exposed population. Relative risk for genotype combined with radiation dose (RR2 in Table III) showed that risk for the *Long* genotype increased with increasing radiation dose (RR: 1.76, 95%CI: 0.88–3.53 for 5–712 mGy and RR: 2.60, 95%CI: 1.36–4.96 for ≥712 mGy), whereas that for the *Short* genotype remained unchanged (RR: 2.11, 95%CI: 1.09–4.08 for <5 mGy and RR: 2.45, 95%CI: 1.22–4.92 for ≥712 mGy) independently of radiation exposure status or dose, resulting in almost identical relative risks for both genotypes at the highest dose.

Finally, we extended the analysis to histological type of lung cancer (adenocarcinoma or squamous cell carcinoma). With lung adenocarcinoma, there was a significant increase in risk for the *Short* genotype only in the non-exposed population (RR: 3.33, 95% CI: 1.23–9.02, Table IV) as well as a radiation-associated elevation in risk for the *Long* genotype (RR: 4.37, 95% CI: 1.72–11.1 for ≥712 mGy). With lung squamous cell carcinoma, there were no significant risk differences among these genotypes (data not shown).

Table II. Association between CA repeat polymorphism and lung cancer risk

Genotype	N[a], cases/sub-cohort	RR[b]	95% CI[c]
Long	57/1176	1.0[d]	
Short	56/890	1.79	1.14–2.82

[a]Eleven cases and 78 sub-cohort members were excluded due to lack of information about an adjustment factor.
[b]RR: relative risks adjusted for age, gender, city, smoking and radiation dose.
[c]95% confidence interval.
[d]The genotype serves as reference category.

Table III. CA repeat polymorphism and lung cancer risk among radiation dose-stratified populations

Genotype	N[a], cases/sub-cohort	RR1[b]	95% CI[c]	RR2[d]	95% CI[c]
Non-exposed					
Long	15/488	1.0[e]		1.0[e]	
Short	22/389	2.43	1.23–4.79	2.11	1.09–4.08
5–712 mGy[f]					
Long	18/343	1.0[e]		1.76	0.88–3.53
Short	17/256	1.27	0.65–2.47	2.24	1.11–4.49
≥712 mGy[f]					
Long	24/345	1.0[e]		2.60	1.36–4.96
Short	17/245	0.92	0.49–1.72	2.45	1.22–4.92

[a]Eleven cases and 78 sub-cohort members were excluded due to lack of information about an adjustment factor.
[b]RR1: genetic relative risks, *Short* versus *Long* genotype, adjusted for age, gender, city and smoking.
[c]95% confidence interval
[d]RR2: genetic and radiation-related risks, with reference to non-exposed *Long* genotype.
[e]Reference category.
[f]712 mGy: median dose in exposed sub-cohort members.

Discussion

We investigated the association between CA repeat number polymorphism in the *EGFR* gene and lung cancer risk using a case–cohort study setting, with the aim of elucidating risk of radiation-associated lung cancer in individuals with different *EGFR* genotypes. In the radiation dose-stratified analysis, we found that the *Short* genotype (the smaller sums of CA repeat numbers of two alleles) was significantly associated with an increased risk of lung cancer in survivors who had not been exposed to radiation (Table III). When we further examined the risk of lung cancer by histological types, adenocarcinoma, but not squamous cell carcinoma, showed a significant association between CA repeat genotypes (*Long* and *Short*) and lung cancer risk (Table IV). That is consistent with the clinico-pathological observation that adenocarcinoma is the most frequent histology in lung cancer of non-smokers, with frequent *EGFR* mutations detected

Table IV. CA repeat polymorphism and lung cancer risk with adenocarcinoma histology among radiation dose-stratified populations

Genotype	*N*, cases/sub-cohort	RR1[a]	95% CI[b]	RR2[c]	95% CI[b]
Non-exposed					
Long	6/488	1.0[d]		1.0[d]	
Short	13/389	3.33	1.23–9.02	2.93	1.11–7.73
5–712 mGy[e]					
Long	9/343	1.0[d]		2.18	0.77–6.17
Short	6/256	0.94	0.34–2.66	2.02	0.65–6.31
≥712 mGy[e]					
Long	17/345	1.0[d]		4.37	1.72–11.1
Short	9/245	0.72	0.32–1.61	3.20	1.13–9.00

[a]RR1: genetic relative risks, *Short* versus *Long* genotype, adjusted for age, gender, city and smoking.
[b]95% confidence interval.
[c]RR2: genetic and radiation-related risks, with reference to non-exposed *Long* genotype.
[d]Reference category.
[e]712 mGy: median dose in exposed sub-cohort members.

(30–50%) (31). The results suggest that the *EGFR* CA repeat number polymorphism may work as an indicator of individuals susceptible to lung cancer, specifically adenocarcinoma, in the Japanese population who have not been exposed to ionizing radiation. One limitation of this study is that no information about the *EGFR* mutation status of the cases was available. Population-based risk estimation of *EGFR*-mutated lung cancer for the CA repeat number polymorphism is therefore a goal of future research. Interestingly, the shorter CA repeat length has been reported to be associated with *EGFR* mutations among lung adenocarcinoma patients (23).

When looking at radiation dose effects on lung cancer risk, A-bomb survivors with the *Long* genotype were found to have a significant elevation of lung cancer risk that increased with increasing radiation dose, whereas the risk among those with the *Short* genotype did not change with radiation dose (Tables III and IV). As a result, the differences in risk between the *Long* and *Short* genotypes decreased with increasing radiation dose. Compared with the *Short* genotype, the *Long* genotype, presumably possessed by more than half of the Japanese population, is hypothesized to confer increased susceptibility to lung cancer after radiation exposure, although the baseline risk at no radiation dose is lower than that with the *Short* genotype. Our findings imply that individuals with the *Long* genotype, who are genetically at low risk of lung cancer when they are not exposed to radiation, may have to be more cautious about medical or occupational radiation exposure to minimize the cancer risk, which would otherwise show an elevation due to their high sensitivity to radiation.

We attempted two different methods of summarizing genotypes: summing CA repeat numbers of two alleles in each individual (resulting in *Long* or *Short* genotype) or combining allele-specific genotypes (resulting in *long/long*, *long/short* or *short/short* genotype). Although both methods produced similar results (Tables II–IV compared with supplementary Tables SI–SIII are available at *Carcinogenesis* Online), results from the latter method seem to be less clear, being in part due to an insufficient number of cases, especially of the *short/short* genotype. This also suggests that both alleles may combine to contribute to the risk of lung cancer, not in an allele-specific way (i.e. no preference for a contributory allele). In addition, analyses in this study were based on the weighted skin dose as an approximation for air dose. There were no substantial differences in the relative risks obtained using skin dose and lung dose, as shown by RR2 (2.45, 95% CI: 1.22–4.92, Table III) for *Short* genotype in the highest skin dose group compared with RR2 (2.45, 95% CI: 1.25–4.83) in the highest lung dose group.

Although the precise mechanism linking the CA repeat polymorphism and lung cancer risk remains to be elucidated, the shorter CA repeat length has been reported to be associated with increased *EGFR* transcription activity—supposedly by alteration in the repressor protein binding property (21,22,32)—and also with an increased *EGFR* mutation rate (23). Thus, the increased risk for the *Short* genotype observed in this study for non-exposed individuals may be in part ascribed to the inherent high EGFR production ability. Furthermore, it is probably that there is an undefined transcriptional mechanism that contributes to the more efficient EGFR production in individuals with the *Long* genotype than with the *Short* genotype as radiation dose increases, which results in an elevated lung cancer risk for the *Long* genotype with radiation dose. Further work, including *in vitro* studies, is required to establish the mechanistic link between the CA repeat polymorphism, EGFR production and radiation exposure in lung carcinogenesis.

Supplementary material

Supplementary Tables I–III can be found at http://carcin.oxfordjournals.org/

Funding

RERF Research Protocol 4-04; Ground-based Research Program for Space Utilization, Japan Space Forum; Grant-in-Aid for Scientific Research, Japanese Ministry of Education, Culture, Sports, Science and Technology (21390199 and 20014032); Grant-in-Aid for the 3rd-term Comprehensive 10-year Strategy for Cancer Control, Japanese Ministry of Health, Labour and Welfare (H21-04).

Acknowledgements

The Radiation Effects Research Foundation, Hiroshima and Nagasaki, Japan, is a private non-profit foundation funded by the Japanese Ministry of Health, Labour and Welfare and the US Department of Energy, the latter in part through the National Academy of Sciences.

Conflict of Interest Statement: None declared.

References

1. Jemal,A. *et al.* (2008) Cancer statistics, 2008. *CA Cancer J. Clin.*, **58**, 71–96.
2. Shields,P.G. *et al.* (2000) Cancer risk and low-penetrance susceptibility genes in gene-environment interactions. *J. Clin. Oncol.*, **18**, 2309–2315.
3. Schwartz,A.G. *et al.* (2007) The molecular epidemiology of lung cancer. *Carcinogenesis*, **28**, 507–518.
4. Sun,S. *et al.* (2007) Lung cancer in never smokers—a different disease. *Nat. Rev. Cancer*, **7**, 778–790.
5. Krewski,D. *et al.* (2006) A combined analysis of North American case-control studies of residential radon and lung cancer. *J. Toxicol. Environ. Health A*, **69**, 533–597.
6. Menzler,S. *et al.* (2008) Population attributable fraction for lung cancer due to residential radon in Switzerland and Germany. *Health Phys.*, **95**, 179–189.
7. Preston,D.L. *et al.* (2007) Solid cancer incidence in atomic bomb survivors: 1958-1998. *Radiat. Res.*, **168**, 1–64.
8. Kyoizumi,S. *et al.* (2005) Individual variation of somatic gene mutability in relation to cancer susceptibility: prospective study on erythrocyte glycophorin a gene mutations of atomic bomb survivors. *Cancer Res.*, **65**, 5462–5469.
9. Herbst,R.S. *et al.* (2008) Lung cancer. *N. Engl. J. Med.*, **359**, 1367–1380.
10. Sozzi,G. *et al.* (1991) Cytogenetic abnormalities and overexpression of receptors for growth factors in normal bronchial epithelium and tumor samples of lung cancer patients. *Cancer Res.*, **51**, 400–404.
11. Shigematsu,H. *et al.* (2006) Somatic mutations of epidermal growth factor receptor signaling pathway in lung cancers. *Int. J. Cancer*, **118**, 257–262.
12. Liang,K. *et al.* (2003) The epidermal growth factor receptor mediates radioresistance. *Int. J. Radiat. Oncol. Biol. Phys.*, **57**, 246–254.
13. Brattstrom,D. *et al.* (2004) HER-2, EGFR, COX-2 expression status correlated to microvessel density and survival in resected non-small cell lung cancer. *Acta Oncol.*, **43**, 80–86.
14. Yacoub,A. *et al.* (2006) Radiotherapy-induced signal transduction. *Endocr. Relat. Cancer*, **13** (suppl. 1), S99–S114.

15. Rodemann,H.P. *et al.* (2007) Radiation-induced EGFR-signaling and control of DNA-damage repair. *Int. J. Radiat. Biol.*, **83**, 781–791.
16. Liu,W. *et al.* (2005) A functional common polymorphism in a Sp1 recognition site of the epidermal growth factor receptor gene promoter. *Cancer Res.*, **65**, 46–53.
17. Chi,D.D. *et al.* (1992) Two chromosome 7 dinucleotide repeat polymorphisms at gene loci epidermal growth factor receptor (EGFR) and pro alpha 2 (I) collagen (COL1A2). *Hum. Mol. Genet.*, **1**, 135.
18. Nomura,M. *et al.* (2007) Polymorphisms, mutations, and amplification of the EGFR gene in non-small cell lung cancers. *PLoS Med.*, **4**, e125.
19. Liu,W. *et al.* (2003) Interethnic difference in the allelic distribution of human epidermal growth factor receptor intron 1 polymorphism. *Clin. Cancer Res.*, **9**, 1009–12.
20. Buerger,H. *et al.* (2004) Allelic length of a CA dinucleotide repeat in the egfr gene correlates with the frequency of amplifications of this sequence—first results of an inter-ethnic breast cancer study. *J. Pathol.*, **203**, 545–550.
21. Gebhardt,F. *et al.* (1999) Modulation of epidermal growth factor receptor gene transcription by a polymorphic dinucleotide repeat in intron 1. *J. Biol. Chem.*, **274**, 13176–13180.
22. Buerger,H. *et al.* (2000) Length and loss of heterozygosity of an intron 1 polymorphic sequence of egfr is related to cytogenetic alterations and epithelial growth factor receptor expression. *Cancer Res.*, **60**, 854–857.
23. Sueoka-Aragane,N. *et al.* (2008) Exon 19 of EGFR mutation in relation to the CA-repeat polymorphism in intron 1. *Cancer Sci.*, **99**, 1180–1187.
24. Lee,S.J. *et al.* (2007) No association between dinucleotide repeat polymorphism in intron 1 of the epidermal growth factor receptor gene EGFR and risk of lung cancer. *Cancer Genet. Cytogenet.*, **172**, 29–32.
25. Zhang,W. *et al.* (2007) Association of the EGFR intron 1 CA repeat length with lung cancer risk. *Mol. Carcinog.*, **46**, 372–380.
26. Yamada,M. *et al.* (2004) Noncancer disease incidence in atomic bomb survivors, 1958-1998. *Radiat. Res.*, **161**, 622–632.
27. Sato,T. (1994) Risk ratio estimation in case-cohort studies. *Environ. Health Perspect.*, **102** (suppl. 8), 53–56.
28. Therneau,T.M. *et al.* (1999) Computing the Cox model for case cohort designs. *Lifetime Data Anal.*, **5**, 99–112.
29. Cullings,H.M. *et al.* (2006) Dose estimation for atomic bomb survivor studies: its evolution and present status. *Radiat. Res.*, **166**, 219–254.
30. Amador,M.L. *et al.* (2004) An epidermal growth factor receptor intron 1 polymorphism mediates response to epidermal growth factor receptor inhibitors. *Cancer Res.*, **64**, 9139–9143.
31. Sequist,L.V. *et al.* (2007) Molecular predictors of response to epidermal growth factor receptor antagonists in non-small-cell lung cancer. *J. Clin. Oncol.*, **25**, 587–595.
32. Brandt,B. *et al.* (2006) Mechanisms of egfr gene transcription modulation: relationship to cancer risk and therapy response. *Clin. Cancer Res.*, **12**, 7252–7260.

Received September 3, 2009; revised September 3, 2009; accepted October 8, 2009

Carcinogenesis vol.30 no.12 pp.2042–2046, 2009
doi:10.1093/carcin/bgp257
Advance Access publication October 25, 2009

Common genetic variation in *IGF1*, *IGFBP1* and *IGFBP3* and ovarian cancer risk

Kathryn L.Terry[1,2,*], Shelley S.Tworoger[2,3], Margaret A.Gates[2,3], Daniel W.Cramer[1,2] and Susan E.Hankinson[2,3]

[1]Obstetrics and Gynecology Epidemiology Center, Department of Obstetrics and Gynecology, Brigham and Women's Hospital, 221 Longwood Avenue, Boston, MA 02115, USA, [2]Department of Epidemiology, Harvard School of Public Health, Boston, MA 02115, USA and [3]Channing Laboratory, Department of Medicine, Brigham and Women's Hospital and Harvard Medical School, Boston, MA 02115, USA

*To whom correspondence should be addressed. Tel: +617 732 4895; Fax: +617 732 4899;
Email: kterry@partners.org

Insulin-like growth factor (IGF) 1 and its binding proteins foster cellular proliferation and inhibit apoptosis. *In vitro* studies show that IGF1 increases ovarian cell growth and invasive potential, suggesting a role for the IGF1 pathway in ovarian cancer etiology. We evaluated genetic variation in the *IGF1*, *IGFBP1* and *IGFBP3* genes in relation to ovarian cancer risk by genotyping 29 haplotype-tagging single nucleotide polymorphisms in 1173 cases and 1201 controls from the New England Case–Control (NECC) study and 296 cases and 854 controls from the Nurses' Health Study (NHS). The association of haplotypes and single nucleotide polymorphisms (SNPs) with ovarian cancer was estimated using unconditional (NECC) and conditional (NHS) logistic regression. Additionally, we evaluated the association of SNPs with IGF1, IGF-binding protein (IGFBP) 3 and IGFBP2 plasma levels (n = 380 NHS controls). Our data suggest a decreased risk for women carrying haplotype 2C of the *IGF1* gene [odds ratios (ORs) = 0.82, 95% confidence intervals (CIs) = 0.69–0.98] and an increased risk for women carrying haplotype 1D (OR = 1.41, 95% CI = 1.03–1.94) or 2D (OR = 1.20, 95% CI = 1.01–1.41) in the binding proteins. When evaluated individually, three SNPs in the IGFBPs (rs10228265, rs4988515 and rs2270628) were associated with increased ovarian cancer risk, and several *IGF1* (rs11111285, rs1996656 and rs1019731) and *IGFBP3* (rs2270628, rs2854746 and rs2854744) SNPs were significantly associated with IGF1, IGFBP3 and IGFBP2 plasma levels. Some haplotypes and SNPs in the IGF pathway genes may be associated with ovarian cancer risk; however, these results need to be confirmed. Of particular interest was the *IGFBP3* SNP rs2270628, which was associated with both increased IGF1 plasma levels and higher ovarian cancer risk.

Introduction

Insulin-like growth factor (IGF) 1 and its binding proteins foster cellular proliferation and inhibit apoptosis. Biologic evidence from *in vitro* studies shows that IGF1 increases ovarian cell growth and invasive potential, suggesting a role for the IGF1 pathway in ovarian cancer etiology (1–4). Epidemiologic data regarding plasma IGF1 levels and ovarian cancer risk are conflicting. Two prospective studies observed that plasma IGF1 levels are associated with an increased risk of ovarian cancer among younger women (5,6), whereas data from the Nurses' Health Study (NHS) suggested that plasma IGF1 levels may be inversely associated with ovarian cancer risk (19). With respect to IGF-binding proteins (IGFBPs), the prospective studies agree that there are no clear associations of IGFBP3 and IGFBP2 with ovarian cancer risk (5–8).

Abbreviations: CIs, confidence intervals; FPRP, false-positive report probability; htSNPs, haplotype-tagging single nucleotide polymorphisms; HWE, Hardy–Weinberg Equilibrium; IGF, insulin-like growth factor; IGFBP, IGF-binding protein; NECC, New England Case–Control; NHS, Nurses' Health Study; ORs, odds ratios; SNPs, single nucleotide polymorphisms.

Given that genetic variation in the *IGF1*, *IGFBP1* and *IGFBP3* genes are likely to influence plasma levels of IGF1 (9) and its binding proteins and that genetic variation may be a better measure of exposure over a lifetime than a single plasma measurement, we examined whether genetic variation in *IGF1*, *IGFBP1* and *IGFBP3* was associated with ovarian cancer risk in two large population-based studies [New England Case–Control (NECC) study and NHS].

Materials and methods

Study population

New England Case–Control study. Data and specimens from this NECC study of ovarian cancer come from two enrollment phases (phase 1: 1992–1997 and phase 2: 1998–2002) corresponding to two funding periods. Details regarding case and control enrollment are described elsewhere (10). Briefly, 2347 women residing in eastern Massachusetts or New Hampshire with a diagnosis of incident ovarian cancer were identified through hospital tumor boards and statewide cancer registries. Of these women, 1845 were eligible and 1306 (71% of the eligible cases, 1231 epithelial cases) agreed to participate. Controls were identified through a combination of random digit dialing, drivers' license lists and town resident lists. In the first phase, 421 (72%) of the eligible women identified through random digit dialing agreed to participate and 102 (51%) of the eligible women identified through town resident lists agreed to participate. In the second phase, 1843 potential controls were identified, 1267 were eligible, 546 declined to participate by phone or by mail via an 'opt-out' postcard and 721 (57%) were enrolled. Controls were frequency matched to cases on age and state of residence.

All study participants were interviewed at the time of enrollment about known and suspected ovarian cancer risk factors. To avoid the possible impact of preclinical disease on exposure status, cases were asked about exposures that occurred at least 1 year before diagnosis and controls were asked about exposures that occurred >1 year before the interview date. More than 95% of the participants provided a blood specimen that was separated into plasma, red blood cell and buffy coat components and stored in −80°C freezers.

Nurses' Health Study. The NHS cohort was established in 1976 among 121 700 US female registered nurses aged 30–55 years. Women completed an initial questionnaire and have been followed biennially by questionnaire to update exposure status and disease diagnoses.

In 1989–1990, 32 826 participants submitted a blood sample; details of the collection are described elsewhere (11). All samples have been stored in liquid nitrogen freezers since collection. Follow-up of the NHS blood study cohort was 96.1% in 2006. In 2001–2004, 33 040 additional women provided a buccal cell specimen using a mouthwash protocol; follow-up was 99% through 2006. We extracted DNA from each buccal cell specimen within 1 week of receipt using Qiagen DNA Extraction Kit (Qiagen, Valencia, CA) and stored the DNA at −80°C. These studies were approved by the Committee on the Use of Human Subjects in Research at the Brigham and Women's Hospital.

NHS nested case–control study. We collected information on new diagnoses of ovarian cancer and confirmed each diagnosis using methods described previously (12). For this analysis, we included all cases with a DNA specimen submitted prior to diagnosis (incident cases) plus cases who submitted a DNA specimen within 4 years after diagnosis (prevalent cases). The incident and prevalent cases were similar with respect to stage, histology and survival time (13). All cases were diagnosed prior to 1 June 2004 and had no history of a prior cancer, other than non-melanoma skin cancer.

We randomly selected three controls per case from the study participants with DNA available, no prior bilateral oophorectomy and no history of cancer, other than non-melanoma skin cancer, at the time of case diagnosis. We excluded 27 controls from the analysis due to unavailability of genotyping data (n = 25) or because the participant was later diagnosed with ovarian cancer and was included in the analysis as a case (n = 2). Cases and controls were matched on age, menopausal status at baseline and diagnosis, month of blood collection, time of day of blood draw, fasting status and postmenopausal hormone use at blood draw.

Genotyping methods

We selected *IGF1*, *IGFBP1* and *IGFBP3* haplotype-tagging single nucleotide polymorphisms (htSNPs) identified by the Breast and Prostate Cancer Cohort Consortium (http://ccnt.hsc.usc.edu/MECGenetics/) (9,12,14–16). Their method of htSNP selection has been described elsewhere (17). Briefly, single

Changes of ROS during a Two-day Ultra-marathon Race

Authors

N. Hattori[1], T. Hayashi[2], K. Nakachi[2], H. Ichikawa[3], C. Goto[4], Y. Tokudome[5], K. Kuriki[6], H. Hoshino[7], K. Shibata[8], N. Yamada[9], M. Tokudome[10], S. Suzuki[3], T. Nagaya[1], M. Kobayashi[11], S. Tokudome[3]

Affiliations

Affiliation addresses are listed at the end of the article

Key words
- reactive oxygen species
- ultra-marathon
- oxidative stress
- physical performance

Abstract

To assess oxidative stress (OS) induced by endurance exercise, concentrations of serum reactive oxygen species (ROS) were determined in 70 Japanese male amateur runners completing a two-day ultra-marathon race. Serum ROS levels were analyzed at three time points: before the race (baseline), after the 1st day race (mid-race), and after the 2nd day race (goal) (post-race). The means (SE) of ROS were 151.4(3.7) (U. CARR.), 168.7(4.4), and 156.8(4.4), respectively. Significant positive trends were noted between age and serum ROS concentrations at the three race points ($p<0.05$ for all). After adjusting for age, BMI and average monthly running distance, the baseline serum ROS concentrations were positively associated with completion times of the first-day race, in particular ($p<0.05$), suggesting that the concentrations may predict physical performance. The ROS production increased at mid-race ($p<0.05$), but the levels returned to baseline levels at post-race, indicating that an antioxidant defense system may develop post-race to reduce OS.

accepted after revision
November 28, 2008

Bibliography
DOI 10.1055/s-0028-1112144
Published online:
February 6, 2009
Int J Sports Med 2009; 30:
426–429 © Georg Thieme
Verlag KG Stuttgart · New York
ISSN 0172-4622

Correspondence
S. Tokudome
Public Health
Nagoya City University
Graduate School of Medical
Sciences
Kawasumi-1
Mizuho-cho, Mizuho-ku
467-8601 Nagoya
Japan
Tel.: +81/52/853 81 74
Fax: +81/52/842 38 30
tokudome@
med.nagoya-cu.ac.jp

Introduction

Moderate/vigorous physical exercise results in 10–20 times more oxygen uptake than the resting condition, and electron fluxes into the mitochondria of skeletal muscles are enhanced 100–200 times, which inevitably produce reactive oxygen species (ROS). Strenuous physical exercise subsequently induces ischemia-reperfusion injury, inflammation, and muscle damage in proportion to the intensity of exercise and oxygen consumed [3,26,27]. Although many ROS exist, hydroxy-radical (·OH), alkoxy-radical (·OR) and peroxy-radical (·OOR) are highly detrimental and responsible for oxidative stress (OS) on DNAs [33], cells, and cell membranes [25]. Moreover, they have been implicated in aging [13,16] as well as with the onset/progression of cerebro- and cardio-vascular disease, neuromuscular disease, autoimmune disease, and cancer [30,37,40].

Long-term running like an ultra-marathon race imposes OS on cardio-respiratory functions and skeletal muscles [35]. OS yielded by endurance exercise inevitably contributes to muscular damage, lowers physical performance, and induces fatigue due to destruction of cellular macromolecules such as lipids, proteins, and nucleic acids during physical exercise [21,25,32]. However, regular physical exercise and endurance training confer protection against ROS and improve antioxidant defenses by upregulation of responsible gene expression [20,29,32,33,41]. Regular physical activity has therefore been recommended for health promotion [34,39]. In fact, we formerly noted that levels of urinary 8-hydroxydeoxyguanosine (8-OHdG), a marker of oxidative DNA damage, rose after the 1st day running 40 km, but returned to baseline after the 2nd day running 90 km in non-professional Japanese athletes completing a two-day ultra-marathon race. This suggested that prolonged running causes oxidative DNA damage, but antioxidant repair systems are subsequently induced to protect against OS [28].

We here investigated changes of serum ROS concentrations using the D-Roms test [2,4], which directly assesses total ROS, based on the ability of transition metals to catalyze ·OH ·OR, and ·OOR. We also examined correlations between the serum ROS levels and age, alcohol use, smoking, or average monthly running distance, along with any association between baseline serum ROS concentrations and running performance in men finishing the two-day ultra-marathon race.

Table 1 Serum ROS concentrations at baseline and completion times of two race points according to age.

	Age (years)			
	-44	45–54	55-	
	n=23	n=31	n=16	
serum ROS (U. CARR.)	140.2±3.5*	155.4±3.8	161.7±3.5	<0.005**
completion time of 1st-day race (min)	286.5±11.2	303.8±8.5	299.5±11.9	
completion time of 2nd-day race (min)	747.4±28.6	776.7±20.3	791.6±28.2	
total completion time (min)	1033.8±38.6	1080.5±30	1091±38.9	

*Mean±SE

**p value for regression coefficient

Subjects and Methods

Ultra-marathon race

The ultra-marathon race, as described elsewhere [42], was held in Gifu Prefecture, Japan, July 27–28, 2002. In brief, the race involved running 130 km over two days. The weather was partly cloudy, hot and sultry. On the first day, participants started at 11:00 a.m. and ran approximately 40 km within 6.5 h. At 3:30 a.m. on the second morning, they resumed the race to run about 90 km including climbing up to a mountain lake approximately 1100 m high, then returning to the starting point within 15.5 h.

Subjects and methods

Six weeks prior to the race, we administered a questionnaire by mail to all participants. Of them, 161 male runners agreed to participate in the study and gave written informed consent. The analysis was limited to 70 male runners who completed the entire two-day race. We obtained information on demographic anthropometric and lifestyle characteristics, including age, sex, height, weight, smoking and alcohol drinking habits, and average monthly running distance. No specific instructions, including meals and beverages, were given before or during the race.

Baseline blood samples at rest were collected approximately one-two hours before the first stage. Mid-race and post-race samples were obtained less than three-five minutes after the first stage and the final stage.

Serum ROS concentrations were determined by the D-Roms test, using the FRAS 3 (Diacron, Grosseto, Italy) developed by Alberti [1]. The test directly estimates serum ROS levels resulting in cells as a consequence of respiratory burst in the presence of irons acting as catalyzers. ROS react with the exact same number of alkylamines (N, N-diethyl-para-phenylendiamine) and develop a colored complex showing peak absorbance at 505 nm. The concentrations of the colored complex are directly proportional to the total serum ROS levels [17]. One Carratelli unit (U. CARR.) corresponds to 0.8 mg/L hydrogen peroxide. In brief, 20 µl serum and 1.2 ml buffered solution (R2 reagent) were mixed in a cuvette, and 20 µl chromogen substrate (R1 reagent) was added. After shaking to mix, the cuvette was centrifuged for 1 min at 37 °C and incubated for 5 min at 37 °C. Absorbance at 505 nm was monitored for 3 min. The coefficient of variation of ROS measurements was less than 4.3%.

The study protocol was approved by the Institutional Review Board of Nagoya City University Graduate School of Medical Sciences.

Statistical analysis

Mean values or prevalence of baseline characteristics, serum ROS concentrations, and completion times were calculated according to age group (≤44, 45–54, or ≥55). While the trends were probed by linear regression analysis, an analysis of variance (ANOVA) for repeated measures was adopted for comparison of the mean serum ROS levels at baseline, mid-race, and post-race. Tukey's post hoc multiple t-test was performed to examine differences in the least square means. Statistical significance was set at $p<0.05$.

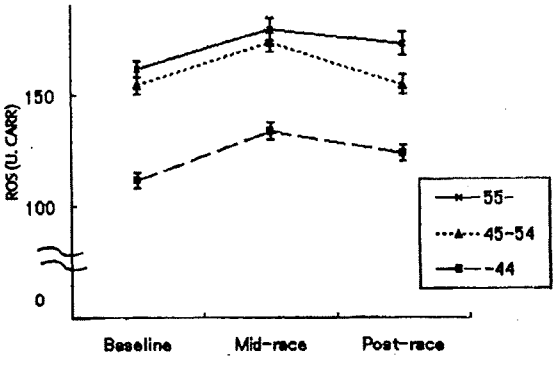

Age	n	Baseline	Mid-race	Post-race
55-	16	161.7±3.5	179.5±5.1*	172.9±5.3
45-54	31	154.4±3.8	173.3±4.3*	154.6±4.3§
-44	23	140.2±3.5	155.2±3.6**	148.5±3.6
All	70	151.4±3.7	168.7±4.4**	156.8±4.4§§

Fig. 1 Changes of serum ROS levels at baseline, mid-race and post-race according to age. Note: Mean±SE, ANOVA for repeated measures was adopted for comparison of the ROS values at baseline (1), mid-race (2) and post-race (3) along with Tukey's post hoc multiple t-test. +$p<0.05$ vs. baseline, ++$p<0.01$ vs. baseline, §$p<0.05$ vs. mid-race, §§$p<0.01$ vs. mid-race.

Results

In all age categories, BMI and percentage of smoking (0–6.5%) were much smaller than those of the general public [42], whereas alcohol consumption (60–75%) was greater (data not shown). Serum ROS levels at baseline were positively related to age ($p<0.005$) (● **Table 1**). Completion times were not significantly related to age, but were positively associated with BMI, and inversely related to average monthly running distance. On the other hand, serum ROS levels were not associated with average monthly running distance. After adjustment for age, BMI and average monthly running distance, baseline serum ROS concentrations were positively related to completion times, after the first-day goal, in particular.

Table 2 Matrices of Pearson's correlation coefficients among serum ROS concentrations, age, BMI, average monthly running distance and completion time.

		Age	BMI	Average monthly running distance	Completion time		
					1st day	2nd day	Total
serum ROS concentrations	baseline	0.33**	0.09	−0.04	0.34**	0.28*	0.30*
	mid-race	0.30*	0.09	0.11	0.16	0.14	0.15
	post-race	0.24*	0.08	−0.01	0.15	0.18	0.17
age			0.04	0.07	0.21	0.20	0.21
BMI				0.07	0.25*	0.27*	0.27*
average monthly running distance					−0.66***	−0.62***	−0.65***
completion time	1st day					0.84****	0.92****
	2nd day						0.98****
	total						
adjusted serum ROS concentrations[a)]	baseline				0.34*	0.23	0.28*

*p<0.05, **p<0.01, ***p<0.0001

a)Adjusted for age, BMI and average monthly running distance

Overall means(SE) of serum ROS levels at baseline, mid-race, and post-race were 151.4(3.7)(U. CARR.), 168.7(4.4), and 156.8(4.4), respectively. The age group-specific serum ROS concentrations at mid-race were universally higher than those at baseline (● **Fig. 1**), and the post-race levels returned to the baseline value. In particular, the group less than 45 years old had lower ROS levels at all race points (● **Table 2**).

Discussion

This is, to our knowledge, the first study of changes in serum ROS concentrations in ultra-marathon runners. Significantly higher serum ROS levels were demonstrated among older than younger runners. Age was not related to completion times; however, there were significant positive correlations between baseline serum ROS concentrations and completion times. Our study also showed apparent elevations of serum ROS levels after the first day running 40 km. However, the values subsequently returned to baseline after the second day running 90 km in spite of double the running distance.

Aging is a critical determining factor for OS [15,18,19,24,32]. Many studies have demonstrated a ROS theory of life span or aging associated with mitochondrial ROS production [25,36], cumulative damage to DNA [23,33], inflammation [32,43] and lipid peroxidation in aged tissues such as skeletal muscle [9,10]. As reported previously, physical exercise may compensate for the elevation in the OS associated with aging [12,38]. In the present study, serum ROS concentrations of all physically trained runners were apparently lower than in their healthy counterparts (250–300 U. CARR.) [2,4]. Serum ROS concentrations adjusted for age, BMI and average monthly running distance were related to completion times, after the first day race, in particular, indicating that serum ROS levels at baseline may predict physical performance, which is compatible with the observations that serum ROS concentrations appear to be associated with anti-oxidant defenses. The runners were exposed to a large quantity of oxygen, and the inevitable increased ROS generation during exercise serves as messenger in exercise-induced adaptive gene expression [7,32]. Elite marathon runners usually have higher maximum oxygen intake (VO_2max) values [6,11,14]. As is the case for VO_2max, serum ROS concentrations may be a key factor in the performance of endurance exercises, including marathon and ultra-marathon running. This may corroborate observations that ROS generation effectively results in lower baseline ROS concentrations, increased activity of antioxidant and damage repair enzymes, and lower oxidative damage levels [31,32]. However, we failed to detect an inverse association between the average monthly running distance and serum ROS levels, which may be partly due to the relatively narrow range of the average monthly running distance among the participants.

We previously observed that concentrations of urinary 8-OHdG elevated after the first stage and returned to baseline level after the second stage [28]. Similarly, we detected concordant changes in serum ROS concentrations in the present study, indicating that exercise-induced serum ROS were potentially attenuated by delayed upregulation in antioxidant gene expression and/or increased enzymatic activity [5,8,24]. Indeed, Kostaropoulos et al. [22] have noted higher catalase activity in long-distance runners than short-distance runners. These observations suggested that prolonged exercise may upregulate an antioxidant defense system to cope with exercise-induced OS.

In conclusion, our study indicated that serum ROS concentrations are associated with age in ultra-marathon runners. Serum ROS levels at baseline appear to predict the physical performance of ultra-marathon runners. We observed that prolonged running increased the serum ROS concentrations after the first day, but returned to baseline after the second day, which may well be due to upregulation of an anti-oxidation system.

Acknowledgements

This study was supported, in part, by a Grant-in-Aid from the Ministry of Education, Culture, Sports, Science, and Technology, Japan. We appreciate the runners having willingly participated in our study and the chairman and organizing committee of the Maranic race. We thank Ms. Fujii, T., Ms. Kubo, Y., Ms. Nakanishi, N., Ms. Ito, Y., Ms. Higuchi, K., and Ms. Watanabe, M. for their technical assistance.

Affiliations

[1] Public Health, Nagoya City University Graduate School of Medical Sciences, Nagoya, Japan

[2] Department of Radiobiology/Molecular Epidemiology, Radiation Effects Research Foundation, Hiroshima, Japan

[3] Department of Health Promotion and Preventive Medicine, Nagoya City University Graduate School of Medical Sciences, Nagoya, Japan

[4] Department of Health and Nutrition, Nagoya Bunri University, Inazawa, Japan
[5] School of Nutritional Sciences, Nagoya University of Arts and Sciences, Nisshin, Japan
[6] Department of Epidemiology and Prevention, Aichi Cancer Center Research Institute, Nagoya, Japan
[7] Department of Health Promotion, Aichi Bunkyo Women's College, Inazawa, Japan
[8] Department of Health Promotion, Kasugai Health Maintenance Center, Kasugai, Japan
[9] Department of Nutrition, Tenshi College, Sapporo, Japan
[10] Medical Center, Yokohama City University, Yokohama, Japan
[11] Department of Musculoskeletal Medicine, Nagoya City University Graduate School of Medical Sciences, Nagoya, Japan

References

1 *Alberti A, Bolognini L, Macciantelli D, Caratelli M.* The radical cation of N, N-diethyl-para-phenylendiamine: a possible indicator of oxidative stress in biological samples. Res Chem Intermed 1999; 26: 253–267
2 *Cesarone MR, Belcaro G, Carratelli M, Cornelli U, Sanctis MT De, Incandela L, Barsotti A, Terranova R, Nicolaides A.* A simple test to monitor oxidative stress. Int Angiol 1999; 18: 127–130
3 *Child RB, Wilkinson DM, Fallowfield JL, Donnelly AE.* Elevated serum antioxidant capacity and plasma malondialdehyde concentration in response to a simulated half-marathon run. Med Sci Sports Exerc 1998; 30: 1603–1607
4 *Cornelli U, Terranova R, Luca S, Cornelli M, Alberti A.* Bioavailability and antioxidant activity of some food supplements in men and women using the D-Roms test as a marker of oxidative stress. J Nutr 2001; 131: 3208–3211
5 *Criswell D, Powers S, Dodd S, Lawler J, Edwards W, Renshler K, Grinton S.* High intensity training-induced changes in skeletal muscle antioxidant enzyme activity. Med Sci Sports Exerc 1993; 25: 1135–1140
6 *Davies CT, Thompson MW.* Aerobic performance of female marathon and male ultramarathon athletes. Eur J Appl Physiol 1979; 41: 233–245
7 *Davies KJ, Quintanilla AT, Brooks GA, Packer L.* Free radicals and tissue damage produced by exercise. Biochem Biophys Res Commun 1982; 107: 1198–1205
8 *Elosua R, Molina L, Fito M, Arquer A, Sanchez-Quesada JL, Covas MI, Ordonez-Llanos J, Marrugat J.* Response of oxidative stress biomarkers to a 16-week aerobic physical activity program, and to acute physical activity, in healthy young men and women. Atherosclerosis 2003; 167: 327–334
9 *Evans W.* Functional and metabolic consequences of sarcopenia. J Nutr 1997; 127: 998S–1003S
10 *Evans WJ, Campbell WW.* Sarcopenia and age-related changes in body composition and functional capacity. J Nutr 1993; 123: 465–468
11 *Farrell PA, Wilmore JH, Coyle EF, Billing JE, Costill DL.* Plasma lactate accumulation and distance running performance. Med Sci Sports 1979; 11: 338–344
12 *Fatouros IG, Jamurtas AZ, Villiotou V, Pouliopoulou S, Fotinakis P, Taxildaris K, Deliconstantinos G.* Oxidative stress responses in older men during endurance training and detraining. Med Sci Sports Exerc 2004; 36: 2065–2072
13 *Flora SJ.* Role of free radicals and antioxidants in health and disease. Cell Mol Biol (Noisy-le-grand) 2007; 53: 1–2
14 *Hagan RD, Smith MG, Gettman LR.* Marathon performance in relation to maximal aerobic power and training indices. Med Sci Sports Exerc 1981; 13: 185–189
15 *Hagihara M, Nishigaki I, Maseki M, Yagi K.* Age-dependent changes in lipid peroxide levels in the lipoprotein fractions of human serum. J Gerontol 1984; 39: 269–272
16 *Halliwell B.* Oxidants and human disease: some new concepts. Faseb J 1987; 1: 358–364
17 *Hayashi I, Morishita Y, Imai K, Nakamura M, Nakachi K, Hayashi T.* High-throughput spectrophotometric assay of reactive oxygen species in serum. Mutat Res 2007; 631: 55–61
18 *Honda Y, Honda S.* Oxidative stress and life span determination in the nematode Caenorhabditis elegans. Ann N Y Acad Sci 2002; 959: 466–474
19 *Ji LL.* Antioxidant enzyme response to exercise and aging. Med Sci Sports Exerc 1993; 25: 225–231
20 *Knez WL, Jenkins DG, Coombes JS.* Oxidative stress in half and full Ironman triathletes. Med Sci Sports Exerc 2007; 39: 283–288
21 *Konig D, Wagner KH, Elmadfa I, Berg A.* Exercise and oxidative stress: significance of antioxidants with reference to inflammatory, muscular, and systemic stress. Exerc Immunol Rev 2001; 7: 108–133
22 *Kostaropoulos IA, Nikolaidis MG, Jamurtas AZ, Ikonomou GV, Makryglannis V, Papadopoulos G, Kouretas D.* Comparison of the blood redox status between long-distance and short-distance runners. Physiol Res 2006; 55: 611–616
23 *Lee BM, Kwack SJ, Kim HS.* Age-related changes in oxidative DNA damage and benzo(a)pyrene diolepoxide-I (BPDE-I)-DNA adduct levels in human stomach. Toxicol Environ Health A 2005; 68: 1599–1610
24 *Leeuwenburgh C, Fiebig R, Chandwaney R, Ji LL.* Aging and exercise training in skeletal muscle: responses of glutathione and antioxidant enzyme systems. Am J Physiol 1994; 267: R439–445
25 *Leeuwenburgh C, Heinecke JW.* Oxidative stress and antioxidants in exercise. Curr Med Chem 2001; 8: 829–838
26 *Mastaloudis A, Morrow J, Hopkins D, Devaraj S, Traber M.* Antioxidant supplementation prevents exercise-induced lipid peroxidation, but not inflammation, in ultramarathon runners. Free Radic Biol Med 2004; 36: 1329–1341
27 *Mastaloudis A, Traber MG, Carstensen K, Widrick JJ.* Antioxidants did not prevent muscle damage in response to an ultramarathon run. Med Sci Sports Exerc 2006; 38: 72–80
28 *Miyata M, Kasai H, Kawai K, Yamada N, Tokudome M, Ichikawa H, Goto C, Tokudome Y, Kuriki K, Hoshino H, Shibata K, Suzuki S, Kobayashi M, Goto H, Ikeda M, Otsuka T, Tokudome S.* Changes of urinary 8-hydroxydeoxyguanosine levels during a two-day ultramarathon race period in Japanese non-professional runners. Int J Sports Med 2008; 29: 27–33
29 *Miyazaki H, Oh-ishi S, Ookawara T, Kizaki T, Toshinai K, Ha S, Haga S, Ji LL, Ohno H.* Strenuous endurance training in humans reduces oxidative stress following exhausting exercise. Eur J Appl Physiol 2001; 84: 1–6
30 *Papatheodorou L, Weiss N.* Vascular oxidant stress and inflammation in hyperhomocysteinemia. Antioxid Redox Signal 2007; 9: 1941–1958
31 *Radak Z, Chung HY, Goto S.* Exercise and hormesis: oxidative stress-related adaptation for successful aging. Biogerontology 2005; 6: 71–75
32 *Radak Z, Chung HY, Koltai E, Taylor AW, Goto S.* Exercise, oxidative stress and hormesis. Ageing Res Rev 2008; 7: 34–42
33 *Radak Z, Pucsuk J, Boros S, Josfai L, Taylor AW.* Changes in urine 8-hydroxydeoxyguanosine levels of super-marathon runners during a four-day race period. Life Sci 2000; 66: 1763–1767
34 *Reinehr T, Sousa G de, Toschke AM, Andler W.* Long-term follow-up of cardiovascular disease risk factors in children after an obesity intervention. Am J Clin Nutr 2006; 84: 490–496
35 *Sanchez LD, Corwell B, Berkoff D.* Medical problems of marathon runners. Am J Emerg Med 2006; 24: 608–615
36 *Schriner SE, Linford NJ, Martin GM, Treuting P, Ogburn CE, Emond M, Coskun PE, Ladiges W, Wolf N, Remmen H Van, Wallace DC, Rabinovitch PS.* Extension of murine life span by overexpression of catalase targeted to mitochondria. Science 2005; 308: 1909–1911
37 *Selfried HE, Anderson DE, Fisher EI, Milner JA.* A review of the interaction among dietary antioxidants and reactive oxygen species. J Nutr Biochem 2007; 18: 567–579
38 *Sial S, Coggan AR, Hickner RC, Klein S.* Training-induced alterations in fat and carbohydrate metabolism during exercise in elderly subjects. Am J Physiol 1998; 274: E785–790
39 *Sims J, Hill K, Davidson S, Gunn J, Huang N.* A snapshot of the prevalence of physical activity amongst older, community dwelling people in Victoria, Australia: patterns across the 'young-old' and 'old-old'. BMC Geriatr 2007; 7: 4
40 *Singh U, Jialal I.* Oxidative stress and atherosclerosis. Pathophysiology 2006; 13: 129–142
41 *Taddei S, Galetta F, Virdis A, Ghiadoni L, Salvetti G, Franzoni F, Giusti C, Salvetti A.* Physical activity prevents age-related impairment in nitric oxide availability in elderly athletes. Circulation 2000; 101: 2896–2901
42 *Tokudome S, Kuriki K, Yamada N, Ichikawa H, Miyata M, Shibata K, Hoshino H, Tsuge S, Tokudome M, Goto C, Tokudome Y, Kobayashi M, Goto H, Suzuki S, Okamoto Y, Ikeda M, Sato Y.* Anthropometric, lifestyle and biomarker assessment of Japanese non-professional ultra-marathon runners. J Epidemiol 2004; 14: 161–167
43 *Yao H, Edirisinghe I, Yang SR, Rajendrasozhan S, Kode A, Caito S, Adenuga D, Rahman I.* Genetic ablation of NADPH oxidase enhances susceptibility to cigarette smoke-induced lung inflammation and emphysema in mice. Am J Pathol 2008; 172: 1222–1237

reprints from

Cellular Immunology

Cellular Immunology
Vol. 255, Issue 1-2, pp 61-68, 2009

Caspase-independent cell death without generation of reactive oxygen species in irradiated MOLT-4 human leukemia cells

by
Kengo Yoshida, Yoshiko Kubo, Yoichiro Kusunoki, Yukari Morishita, Hiroko Nagamura, Ikue Hayashi, Seishi Kyoizumi, Toshio Seyama, Kei Nakachi, Tomonori Hayashi

ELSEVIER

Elsevier
Radarweg 29
1043 NX Amsterdam
The Netherlands
Tel: +31 (0)20 485 3440
Fax: +31 (0)20 485 3280

Cellular Immunology 255 (2009) 61–68

Contents lists available at ScienceDirect

Cellular Immunology

journal homepage: www.elsevier.com/locate/ycimm

Caspase-independent cell death without generation of reactive oxygen species in irradiated MOLT-4 human leukemia cells

Kengo Yoshida [a], Yoshiko Kubo [a], Yoichiro Kusunoki [a], Yukari Morishita [a], Hiroko Nagamura [a], Ikue Hayashi [b], Seishi Kyoizumi [a,c], Toshio Seyama [d], Kei Nakachi [a], Tomonori Hayashi [a,*]

[a] Department of Radiobiology/Molecular Epidemiology, Radiation Effects Research Foundation, 5-2 Hijiyama Park, Minami-ku, Hiroshima 732-0815, Japan
[b] Central Research Laboratory, Hiroshima University Faculty of Dentistry, Hiroshima, Japan
[c] Faculty of Human Ecology, Yasuda Women's University, Hiroshima, Japan
[d] Faculty of Pharmaceutical Sciences, Yasuda Women's University, Hiroshima, Japan

ARTICLE INFO

Article history:
Received 5 September 2008
Accepted 23 October 2008
Available online 9 December 2008

Keywords:
Apoptosis
Caspase
Immune cells
Ionizing radiation
Necrosis
Reactive oxygen species

ABSTRACT

To improve our understanding of ionizing radiation effects on immune cells, we investigated steps leading to radiation-induced cell death in MOLT-4, a thymus-derived human leukemia cell. After exposure of MOLT-4 cells to 4 Gy of X-rays, irradiated cells sequentially showed increase in intracellular reactive oxygen species (ROS), decrease in mitochondrial membrane potential, and eventually apoptotic cell death. In the presence of the caspase inhibitor z-VAD-fmk, irradiated cells exhibited necrotic characteristics such as mitochondrial swelling instead of apoptosis. ROS generation was not detected during this necrotic cell death process. These results indicate that radiation-induced apoptosis in MOLT-4 cells requires elevation of intracellular ROS as well as activation of a series of caspases, whereas the cryptic necrosis program—which is independent of intracellular ROS generation and caspase activation—is activated when the apoptosis pathway is blocked.

1. Introduction

A single cell-death-inducing stimulus such as ionizing radiation seems to evoke multiple and discrete mechanisms of cell death, and the physiological condition of the cells may determine the eventual outcome—whether apoptosis or necrosis, or another type of cell death [1]. Apoptosis and necrosis reveal varying postmortem features based on morphology, molecular events, and metabolic variations [2]. Immune responses to these two types of cell death may also differ in the event of radiation exposure including cancer radiotherapy (i.e., immune suppression in apoptosis vs. potent immune responses and inflammation in necrosis). Thus, elucidation of the cell-death mechanisms is essential to an improved understanding of radiation effects on a host. Early intracellular responses to radiation such as the possible involvement of reactive oxygen species (ROS)[1] in the process of apoptosis and/or necrosis, may determine the fate of irradiated cells and will be of particular interest in prevention and treatment of radiation-induced insults.

Apoptotic cell death is an active, programmed process of cell dismantling, which occurs under normal physiological and pathological conditions. Apoptotic features include chromatin condensation and fragmentation, overall cell shrinkage, formation of condensed cell bodies (apoptotic bodies), and minor changes in the cytoplasmic organelles. The molecular pathways of apoptosis, in which a series of cysteine proteases known as caspases play a central role, have been extensively studied over the last decade [3–5], but the upstream initiating events of radiation-induced apoptosis as well as the roles of mitochondria and ROS in these pathways remain to be elucidated [6].

Necrosis has thus far been considered passive and accidental cell death caused by extreme environmental perturbation, and characterized by plasma membrane rupture and swelling of the cytoplasmic organelles, particularly mitochondria. However, our current knowledge of what happens in the molecular pathways of radiation-induced necrosis is very limited. Recent studies using various cell types have shown that blockage of the apoptosis pathways failed to prevent cell death and instead led to necrotic cell death, which implies that necrosis is a physiologically alternative process of cellular dismantling under particular conditions [7–9].

Therefore, we investigated radiation-induced intracellular events, particularly ROS generation, to their conclusion in apoptosis or necrosis, using MOLT-4 cells with or without a caspase inhibitor z-VAD-fmk. Our results show that a 4 Gy X-ray irradiation mainly induced apoptotic cell death in MOLT-4 cells, but resulted in necrotic cell death in the presence of z-VAD-fmk. Moreover, generation of intracellular ROS was observed during the apoptotic

* Corresponding author. Fax: +81 82 261 3170.
E-mail address: tomo@rerf.or.jp (T. Hayashi).

[1] *Abbreviations used:* PI, propidium iodide; ROS, reactive oxygen species; z-VAD-fmk, *N*-benzyloxycarbonyl-Val-Ala-Asp-fluoromethylketone.

0008-8749/$ - see front matter © 2008 Elsevier Inc. All rights reserved.
doi:10.1016/j.cellimm.2008.10.006

process of irradiated MOLT-4 cells but not during the necrotic process of these cells pretreated with z-VAD-fmk: It is therefore possible that radiation may induce necrotic cell death through ROS-independent pathways.

2. Materials and methods

2.1. Cell culture

Human leukemia T cell line MOLT-4 [10] was obtained from the Japanese Cancer Resources Bank (Tokyo, Japan) and was grown in RPMI 1640 medium supplemented with 10% fetal calf serum (FCS), L-glutamine (2 mM), penicillin (100 units/ml), and streptomycin (100 μg/ml) in a 5% CO_2 humidified atmosphere. All experiments were performed with cells in the exponential growth phase.

2.2. Irradiation

Irradiation of cells was performed using an X-ray generator (Shimadzu HF-320; 220 kVp, 8 mA) with a 0.5 mm aluminum and 0.3 mm copper filter at a dose rate of approximately 0.8 Gy/min. Cells in the exponential growth phase were irradiated in RPMI 1640 with 10% FCS in a plastic dish at room temperature under normal oxygen tension.

2.3. Mitochondrial membrane potential and superoxide anions

To measure mitochondrial membrane potential ($\Delta\psi m$) and generation of the superoxide anions $O_2^{\cdot-}$, cells (5×10^5) were stained with 0.26 μM Rhodamine123 (Rh123; Molecular Probes, Eugene, OR) and 20 μM hydroethidine (HE; Molecular Probes), respectively, for 20 min at 37 °C [11–15]. Cells were washed once with phosphate buffered saline (PBS) containing 1% FCS, and then analyzed with a FACScan flow-cytometer (BD Biosciences, Franklin Lakes, NJ). To isolate certain cell fractions, cells were sorted using a FACS Vantage SE (BD Biosciences).

2.4. Phosphatidyl serine externalization and cell death

Externalization of the plasma membrane phosphatidyl serine, an early process of apoptosis, and cell death were assessed by measuring annexin V-FITC- and propidium iodide (PI)-stained cells, respectively, using a kit from MBL (Nagoya, Japan). After incubation in the reaction buffer (130 μl of binding buffer, 0.5 μl of annexin V-FITC, and 1.0 μl of PI) for 10 min, cells were analyzed using a FACScan flow-cytometer.

2.5. Catalytic activity of caspases

To suppress the activity of caspases, cells were pretreated with z-VAD-fmk (*N*-benzyloxycarbonyl-Val-Ala-Asp-fluoromethylketone; Peptide Institute, Osaka, Japan). Cells were suspended in the medium containing 100 μM z-VAD-fmk for 30 min prior to irradiation. Catalytic activity of a series of caspases was determined based on colorimetric assays. Cells (5×10^5) were lysed in lysis buffer (10 mM Tris–HCl, pH 7.4, 25 mM NaCl, 0.25% Triton X-100, 1 mM EDTA). The lysates were centrifuged at 16,000g at 4 °C for 30 min, and the supernatants were stored at −80 °C until analysis. Each supernatant (25 μg) was then incubated with 100 μl of caspase buffer (50 mM HEPES, pH 7.2, 100 mM NaCl, 1 mM EDTA, 10% sucrose, 0.1% CHAPS, 5 mM dithiothreitol) containing 100 μM substrates conjugated with 7-amino-4-methylcoumarin (Ac-VDVAD-AMC for caspase-2, Ac-DNLD-AMC for caspase-3, Ac-DEVD-AMC for caspase-3 and caspase-7, Ac-IETD-AMC for caspase-8, and Ac-LEHD-AMC for caspase-9) at 37 °C for 60 min. The release of 7-amino-4-methylcoumarin was measured using a spectrometer.

2.6. Cytochrome c release from mitochondria

Flow-cytometry was used to analyze cytochrome *c* release from mitochondria, as reported by Stahnke et al. [16]. Briefly, irradiated cells were fixed and permeabilized with 4% paraformaldehyde and 0.2% saponin for 20 min at 4 °C, and washed twice with Perm/Wash Buffer including fetal bovine serum, sodium azide, and saponin (BD Biosciences). Cells were incubated with 5 μg/ml mouse IgG to block nonspecific binding. Anti-cytochrome c antibody (1:20, clone 7H8.2C12, BD Biosciences) was then added, and cells were incubated at 4 °C for 20 min. Finally, cells were treated with goat anti-mouse IgG-FITC (1:20, Southern Biotech, Birmingham, AL) at 4 °C for 20 min and subjected to a FACScan flow-cytometer.

2.7. Transmission electron microscopy

Prefixation was performed with 2% glutaraldehyde in 100 mM cacodylate buffer, followed by washing in 100 mM cacodylate buffer overnight and subsequent postfixation with 2% osmium tetroxide in distilled water for 3 h. Cells were then dehydrated through a graded series of ethanol before being embedded in gelatin capsule with epoxy resin. Samples were sectioned into ultrathins (70–80 nm) using a LKB-8800 ultramicrotome (LKB, Bromma, Sweden), stained with 2% uranyl acetate in distilled water for 10 min and with lead staining solution for 5 min, and then examined using a JEM-2000EX (JEOL, Tokyo, Japan).

3. Results

3.1. Radiation-induced apoptotic cell death of MOLT-4 is characterized by decrease in mitochondrial membrane potential along with increase in intracellular ROS

Since a number of previous studies showed the crucial roles of mitochondria and ROS generation during apoptotic cell death by various stimuli [17–19], we first examined levels of mitochondrial membrane potential ($\Delta\psi m$) and intracellular superoxide anions (ROS) in X-ray-irradiated MOLT-4 cells. At 16 h after a 4 Gy irradiation, membrane potentials of irradiated cells had significantly decreased compared with those in unirradiated cells (Fig. 1A), while most irradiated cells showed elevated intracellular ROS (Fig. 1B). The irradiated MOLT-4 cells also exhibited several apoptotic features, including externalization of plasma membrane phosphatidyl serine (data not shown) and retention of normal mitochondrial shapes (Fig. 2B).

We next investigated temporal changes in irradiated MOLT-4 cells, focusing on mitochondrial membrane potential and intracellular ROS. Flow-cytometric analysis of MOLT-4 cells at 16 h after a 4 Gy irradiation identified five cell fractions (Fig. 3A): a fraction identical to unirradiated cells or viable cell fraction (R1), a low-ROS generating fraction (R2), a high-ROS generating fraction (R3), a moderate-to-high-ROS generating and low-$\Delta\psi m$ fraction (R4), and a low-ROS and low-$\Delta\psi m$ fraction (R5). Because almost all cells in the R4 and R5 fractions were stained with PI, they were considered dying or dead cells (data not shown). To elucidate the sequential process of radiation-induced cell death of MOLT-4, at 16 h after the irradiation we separated all fractions using a cell sorter and then cultured them for additional 8 h before analyzing them again by flow-cytometry. The cells that were in the R1 fraction (Fig. 3A) scattered and were found in R2, R3, R4, and R5 (Fig. 3B-R1). In a similar manner, cells in R3 remained

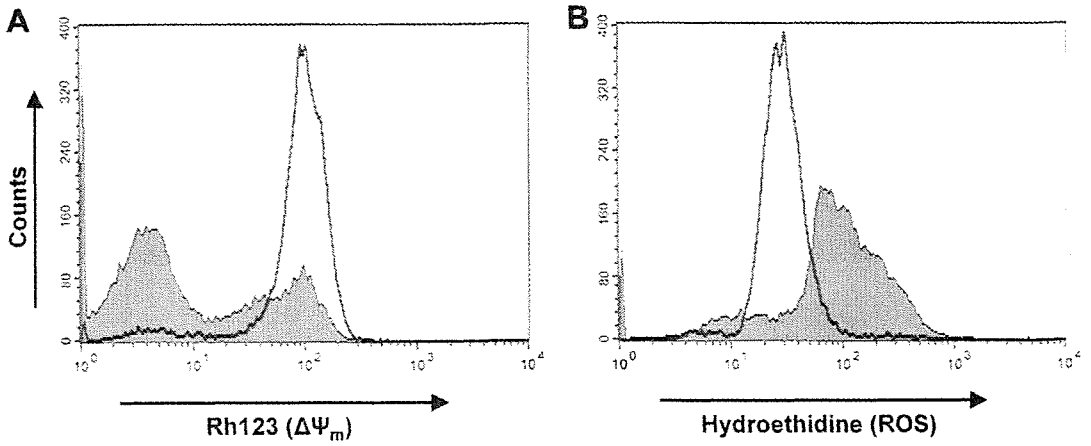

Fig. 1. Mitochondrial membrane potential and intracellular ROS in irradiated MOLT-4 cells. MOLT-4 cells were analyzed by flow-cytometry at 16 h after a 4 Gy X-ray irradiation. (A) Signal intensity of Rhodamine123 (Rh123), reflecting the membrane potential (Δψm), decreased in irradiated MOLT-4 cells (shaded histogram) compared with that in unirradiated cells (open histogram). (B) Hydroethidine signals represent levels of intracellular superoxide anions. The signals of irradiated cells (shaded histogram) were elevated, compared with those of unirradiated cells (open histogram).

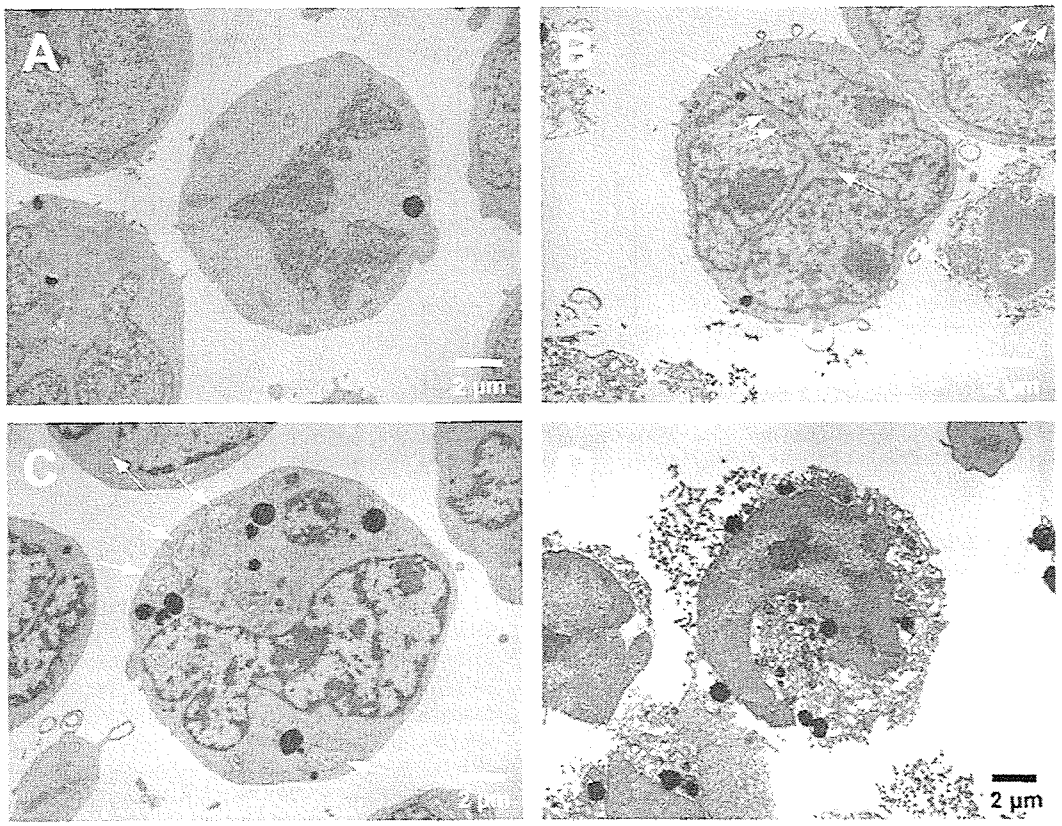

Fig. 2. Cellular morphology of irradiated MOLT-4 cells under the electron microscope. (A) Unirradiated MOLT-4 cells. (B) Irradiated MOLT-4 cells in the low-Δψm R4 fraction. Normal-shaped mitochondria (indicated by white arrows) were observed at 16 h after a 4 Gy irradiation. (C and D) Irradiated MOLT-4 cells pretreated with 100 μM z-VAD-fmk in the low-ROS R2 and low-Δψm R4 fractions, respectively. Swollen mitochondria (indicated by arrows) were observed at 16 h after a 4 Gy irradiation. Scale bar, 2 μm.

in R3 or moved to R4 and R5 (Fig. 3B-R3) and cells in R4 remained in R4 or moved to R5 (Fig. 3B-R4). However, cells in R2 moved only to R4 or remained in R2 (Fig. 3B-R2). It follows that most irradiated MOLT-4 cells may shift from R1 to R3, next to R4, and finally to R5; on the other hand, cells in R2 may shift to R4, and eventually R5. These observations suggest that generation of intracellular ROS is a step before a reduction of mitochondrial membrane potential in the radiation-induced apoptotic process of MOLT-4 cells.

3.2. Radiation-induced necrotic cell death of MOLT-4 without increase in intracellular ROS in the presence of a caspase inhibitor

We next investigated the involvement of caspases in X-ray-induced cell death of MOLT-4 using a broad-range caspase inhibitor, z-VAD-fmk. In the absence of z-VAD-fmk, living cell percentage of irradiated MOLT-4 cells (i.e., the cells not stained with PI) and the cell percentage of the R1 fraction were 20% and 15%, respectively, at 16 h after a 4 Gy irradiation (Fig. 4A-b, A-e, and B). In the pres-

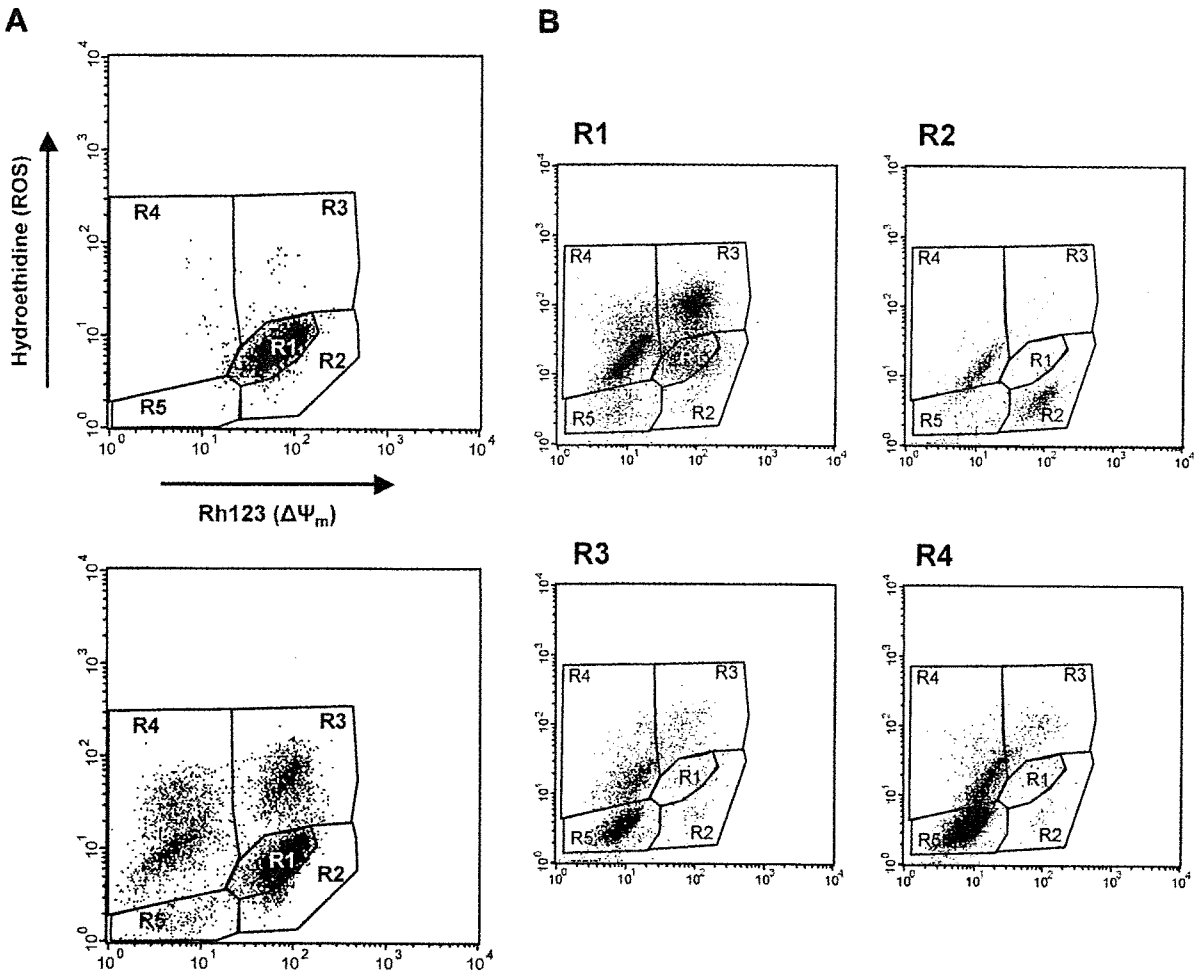

Fig. 3. Temporal changes in irradiated MOLT-4 in terms of mitochondrial membrane potential and intracellular ROS. (A) Upper and lower panels show non-irradiated control and irradiated cells, respectively. In the lower panel, five cell fractions were identified at 16 h after a 4 Gy irradiation: a viable cell fraction (R1), a low-ROS fraction (R2), a high-ROS fraction (R3), a moderate-to-high ROS and low-$\Delta\psi$m fraction (R4), and a low-ROS and low-$\Delta\psi$m fraction (R5). (B) Scattered pattern of cells in each fraction in Fig. 3A after a lapse of another 8 h. Cells in R1, R2, R3, and R4 fractions in the lower panel of Fig. 3A were isolated, cultured for another 8 h, and analyzed again by flow-cytometry.

ence of the caspase inhibitor, the percentages of living cell and the R1 fraction were 75% and 50%, respectively (Fig. 4A-c, A-f, and C). After irradiation with the z-VAD-fmk pretreatment, a number of cells were found in the R4 and R5 fractions (Fig. 4A-c), showing that cell death still occurred after caspase inhibition. Furthermore, in the case of irradiation with z-VAD-fmk, more viable cells were found in the low-ROS R2 fraction than in the high-ROS R3 fraction (Fig. 4A-c), implying that cell death occurs without excess generation of intracellular ROS. In addition, the cells in the low-ROS R2 fraction were considered to be viable, since they were not stained with PI (Fig. 4A-f).

3.3. Time-course analyses of irradiated MOLT-4 cells in the absence or presence of a caspase inhibitor

The time-course analysis clearly shows that irradiated MOLT-4 cells shifted from the R1 fraction to the partially low-ROS R2 or predominantly high-ROS R3 fraction, and eventually to the low-$\Delta\psi$m R4 and R5 fractions (Fig. 4B). On the other hand, cells pretreated with z-VAD-fmk traveled a different course from R1 to low-ROS R2, and eventually to low-$\Delta\psi$m R4 and R5, with no cells going to high-ROS R3 (Fig. 4C). In fact, when the cells in R2 were isolated and their temporal changes were analyzed by flow-cytometry, the R2 cells eventually died via R4 and R5, not R3 (data not shown).

3.4. Suppression of caspase activities by z-VAD-fmk

To confirm the suppressive effects of z-VAD-fmk in irradiated MOLT-4 cells, we next examined catalytic activity of caspases by using colorimetric substrates that mimic the cleavage sites of caspases. In the absence of z-VAD-fmk, activities of caspases—including caspase-3—were clearly enhanced by irradiation and peaked at 8 h after irradiation (Fig. 5). Up-regulation of caspase-3 expression was also confirmed by Western blotting (data not shown). In contrast, the presence of z-VAD-fmk effectively suppressed activities of all caspases examined (Fig. 5). These results were consistent with previous studies [8,20,21] which reported that caspase-3 and other caspases were activated in MOLT-4 cells following ionizing radiation. The results again demonstrated that cell death of irradiated MOLT-4 with z-VAD-fmk was independent of caspase activation.

3.5. Apoptotic and necrotic features related to cellular morphology and the cytochrome c release

We further characterized cell death in irradiated MOLT-4 with transmission electron microscopy, since its morphologic description remains the best way to discriminate apoptosis and necrosis [22]. After cells in each fraction separated with Rh123- and hydroethidine-staining were sorted, an electron microscopic review was performed. In the absence of z-VAD-fmk, mitochondria of irradi-

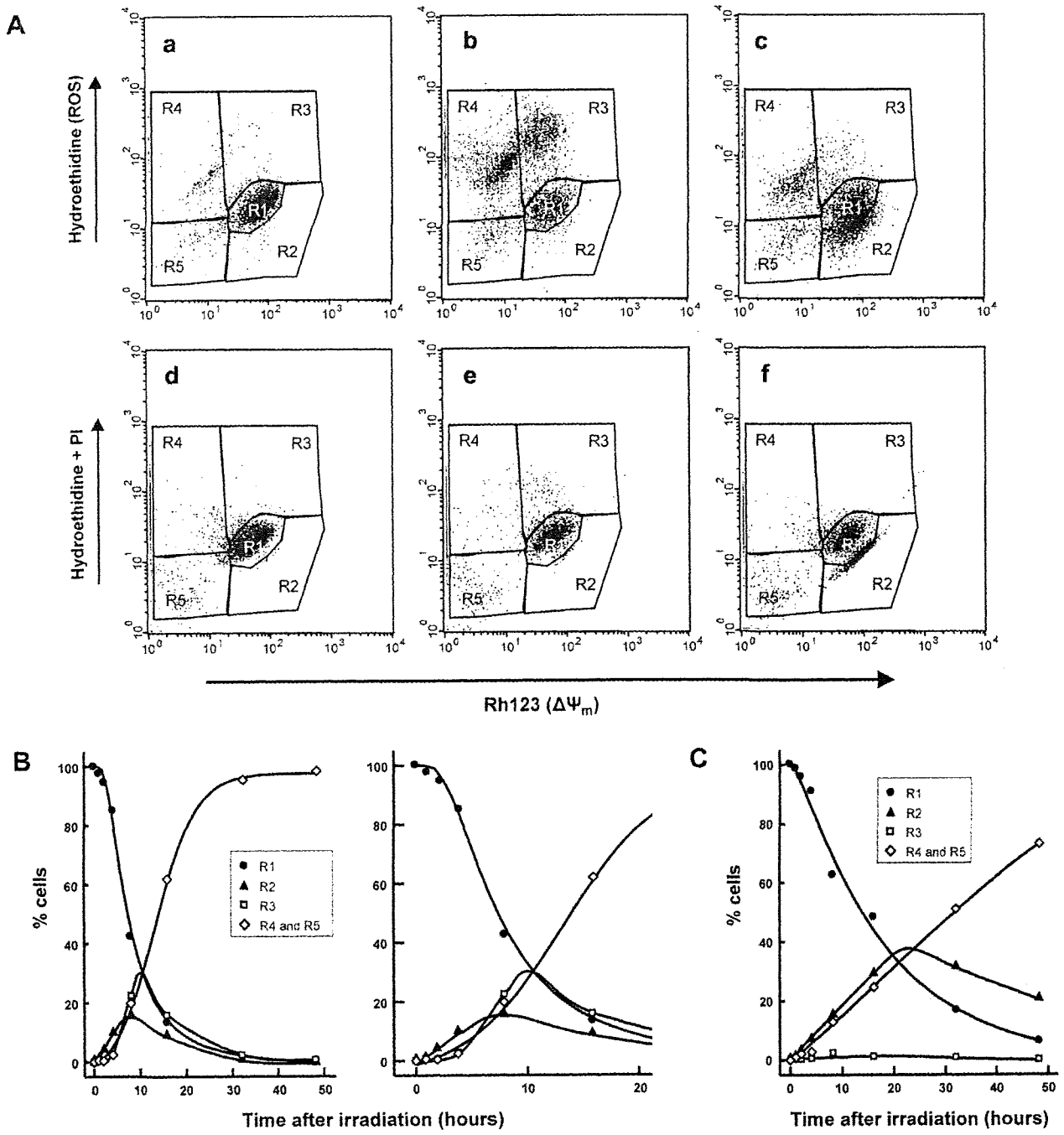

Fig. 4. Effects of caspase inhibition on radiation-induced cell death in MOLT-4. (A) Upper panels show flow-cytometric analyses with Rh123- and hydroethidine-staining on (a) unirradiated MOLT-4 cells, (b) cells at 16 h after a 4 Gy irradiation, and (c) irradiated cells pretreated with 100 μM z-VAD-fmk (note that many cells are located in the low-ROS R2 fraction). Lower panels show PI-staining in addition to Rh123- and hydroethidine-staining on (d) unirradiated cells, (e) irradiated cells, and (f) irradiated cells with z-VAD-fmk, corresponding to panels a, b, and c, respectively. In the lower panels, most PI-stained cells moved out of the displayed region due to their intense signals. (B) Time-course analyses of cells in R1 (viable cells, indicated by circle), R2 (low-ROS, triangle), R3 (high-ROS, square), and R4 and R5 (low-Δψm, rhombus) fractions after a 4 Gy irradiation. An enlarged illustration of the left panel from 0 to 20 h is shown in the right panel. (C) Time-course analyses of cells after a 4 Gy irradiation with a pretreatment with 100 μM z-VAD-fmk. Each cell fraction in Fig. 4B and C corresponds to a fraction in the upper panels of Fig. 4A.

ated MOLT-4 cells—even those in the low-Δψm R4 fraction—retained their normal shapes as already described (Fig. 2B). On the other hand, the organelles were swollen in the low-ROS R2 fraction in the presence of z-VAD-fmk (Fig. 2C). Those observations reinforced the concept that irradiated MOLT-4 cells ended in apoptosis when mediated by caspases, and necrosis proceeded under caspase inhibition. Finally, we examined cytochrome *c* release from mitochondria by flow-cytometry in order to further investigate the molecular mechanisms of radiation-induced necrosis in MOLT-4 cells. Cytochrome *c* release represents a key step in the cell death pathway, and it reportedly plays a role in radiation-induced apoptosis of MOLT-4 cells as well [23]. Cells in viable or early cell death phase, gated according to forward/side scatter properties, were analyzed with anti-cytochrome *c* antibody (clone 7H8.2C12), which binds only to mitochondrial cytochrome *c* [16]. At 16 h after a 4 Gy irradiation, the cytochrome *c* signals were significantly reduced, reflecting the release of cytochrome *c* (Fig. 6B), whereas no obvious changes in cytochrome *c* signals were detected when